Check for updates

Received: 19 July 2019 | Revised: 24 February 2020 | Accepted: 27 February 2020

DOI: 10.1002/mbo3.1031

ORIGINAL ARTICLE

MicrobiologyOpen Open Access WILEY

# Virioplankton distribution in the tropical western Pacific Ocean in the vicinity of a seamount

Yanchu Zhao[1,2,3] | Yuan Zhao[1,2,4] | Shan Zheng[2,4,5] | Li Zhao[1,2,4] | Xuegang Li[1,2,4] | Wuchang Zhang[1,2,4] | Gérald Grégori[6] | Tian Xiao[1,2,4]

[1]CAS Key Laboratory of Marine Ecology and Environmental Sciences, Institute of Oceanology, Chinese Academy of Sciences, Qingdao, China

[2]Laboratory for Marine Ecology and Environmental Science, Qingdao National Laboratory for Marine Science and Technology, Qingdao, China

[3]University of Chinese Academy of Sciences, Beijing, China

[4]Center for Ocean Mega-Science, Chinese Academy of Sciences, Qingdao, China

[5]Jiaozhou Bay Marine Ecosystem Research Station, Institute of Oceanology, Chinese Academy of Sciences, Qingdao, China

[6]Aix-Marseille University, Toulon University, CNRS, IRD, Mediterranean Institute of Oceanography UM110, Marseille, France

**Correspondence**
Yuan Zhao and Tian Xiao, Institute of Oceanology, Chinese Academy of Sciences, 7 Nanhai Rd, Qingdao 266071, China.
Emails: yuanzhao@qdio.ac.cn (Y.Z.); txiao@qdio.ac.cn (T.X.)

**Funding information**
Science & Technology Basic Resources Investigation Program of China, Grant/Award Number: 2017FY100803; National Key Research and Development Program of China, Grant/Award Number: 2017YFA0603204; National Natural Science Foundation of China, Grant/Award Number: 91751202; CNRS-NSFC Joint Research Projects Program, Grant/Award Number: NSFC 41711530149; 2017-2019 Sino-French Cai Yuanpei Programme

## Abstract

The shallow Caroline Seamount is located in the tropical western Pacific Ocean. Its summit is 57 m below the surface and penetrates the euphotic zone. Therefore, it is ideal for the study of the influence of seamount on plankton distribution. Here, virioplankton abundance and distribution were investigated by flow cytometry (FCM) in the Caroline Seamount in August and September 2017. The total abundance of virus-like particles (VLP) was in the range of $0.64 \times 10^6$–$18.77 \times 10^6$ particles/ml and the average was $5.37 \pm 3.75 \times 10^6$ particles/ml. Three to four distinct viral subclusters with similar side scatter but different green fluorescence intensities were identified. Above the deep chlorophyll maximum (DCM), two medium fluorescence virus (MFV) subclusters were discriminated. Between the DCM and the deeper layers, only one MFV subcluster was resolved. In general, low fluorescence viruses (LFV) comprised the most abundant subclusters. In the 75–150 m water column, however, the MFV abundance was higher than the LFV abundance. High fluorescence viruses (HFV) constituted the least abundant subcluster throughout the entire water column. Virioplankton abundance was significantly enhanced at the seamount stations. Environmental factors including water temperature and nitrate concentration were the most correlated with the variation in virioplankton abundance at the seamount stations. Interactions between shallow seamounts and local currents can support large virus standing stocks, causing a so-called indirect "seamount effect" on the virioplankton.

KEYWORDS

Caroline Seamount, flow cytometry, seamount effect, viral subclusters, virioplankton

Yanchu Zhao and Yuan Zhao contributed equally to this work.

This is an open access article under the terms of the Creative Commons Attribution-NonCommercial License, which permits use, distribution and reproduction in any medium, provided the original work is properly cited and is not used for commercial purposes.
© 2020 The Authors. *MicrobiologyOpen* published by John Wiley & Sons Ltd.

## 1 | INTRODUCTION

Viruses are the most abundant entities in marine ecosystems. Their mean abundance is in the range of $10^4$–$10^8$ particles/ml (Wommack & Colwell, 2000). Virioplankton are key ecological drivers in marine biogeochemical processes (Jiao et al., 2010; Suttle, 2007; Suttle, 2016; Weitz & Wilhelm, 2012), and one of the most important top-down controlling agents of prokaryote communities. They account for a significant proportion of bacterial mortality. On a daily basis, they remove 20%–40% of the standing prokaryote stock at the ocean surface (Suttle, 1994) and mitigate up to 80% of prokaryotic production in deep marine environments (Danovaro et al., 2008). By virus-mediated cell lysis, particulate organic matter is transformed into dissolved organic matter, shunting the availability of organic material to higher trophic levels (Suttle, 2007). Viral decay releases carbon, nitrogen, phosphorus, and other nutrients into the surrounding waters, affecting the global marine biogeochemical cycles (Jover, Effler, Buchan, Wilhelm, & Weitz, 2014; Zhang, Wei, & Cai, 2014).

Analyses of viral abundance and distribution help elucidate the roles of these microorganisms in marine biogeochemistry. After high viral abundances were discovered in aquatic environments (Bergh, Børsheim, Bratbak, & Heldal, 1989; Børsheim, Bratbak, & Heldal, 1990), efforts have been made on investigating the abundance and influencing factors of the virus in various marine environments. In general, viruses have relatively lower abundances in oligotrophic regions and the deep sea (De Corte, Sintes, Yokokawa, Reinthaler, & Herndl, 2012; Liang et al., 2017; Winter, Kerros, & Weinbauer, 2009). In contrast, viral abundances are higher in the comparatively more productive coastal areas (Wommack & Colwell, 2000). On average, viruses outnumber their microbial hosts by ~10 times at the surface and up to 16 in the deep ocean (Wigington et al., 2016). Changes in water temperature, salinity, light, nutrient levels, and turbidity may alter viral dynamics and microbial host–virus interactions in marine environments (Mojica & Brussaard, 2014). However, there is relatively little information on virioplankton abundance and distribution in certain marine zones such as seamount ecosystems.

Seamounts are geographically isolated topographic structures that rise >1,000 m from the seafloor (Yesson, Clark, Taylor, & Rogers, 2011). Seamounts are obstacles to ocean circulation and influence hydrological processes by generating internal waves, enhancing internal tides and vertical mixing, forming Taylor columns and eddies, and deflecting isotherms (Read & Pollard, 2017; Roden, 1987; Rogers, 2018; White, Bashmachnikov, Arístegui, & Martins, 2007). These hydrological processes can affect the pelagic communities, causing the so-called "seamount effect" (Dower & Mackas, 1996). This mechanism is reflected in elevated primary production and chlorophyll concentrations over the summits (Boehlert & Genin, 1987; Dower, Freeland, & Juniper, 1992; Genin & Boehlert, 1985). Therefore, seamounts have been hypothesized to be "hotspots" for pelagic biodiversity and productivity (Genin & Dower, 2007).

There are ~30,000 seamounts in the world's oceans (Yesson et al., 2011). However, only ~250–280 of them have been subjected to an extensive biological investigation (Rogers et al., 2015). Seamount topographic structures and summit heights and locations induce various hydrological effects whose relative strength and persistence present with substantial spatiotemporal variation (White et al., 2007). Thus, it is difficult to establish the overall impact of seamounts on biomes. To date, there are very few studies on the pelagic communities in deep-sea seamounts. Moreover, those focused primarily on phytoplankton and zooplankton (Cordeiro, Brandini, Rosa, & Sassi, 2013; Dower & Mackas, 1996; Genin, 2004; Montserrat et al., 2019; Sampaio de Souza, Guimarães da Luz, Macedo, Montes, & Mafalda, 2013; Sonnekus, Bornman, & Campbell, 2017). Further, virioplankton have received the least attention of all members of this microbial community. To the best of our knowledge, only the spatial virioplankton abundance for the Bajo O'Higgins 1 seamount (32°54′S, 73°53′W) has been reported (Chiang & Quiñones, 2007). Viral abundance and production have been explored in the deep-sea sediments around two seamounts at 3,000-m depth in the Tyrrhenian Sea (Danovaro et al., 2009). These limitations of information have rendered it difficult to determine the effects of seamounts on virioplankton distribution. Here, we examined the abundances of virioplankton and their picoplankton hosts in the Caroline Seamount of the tropical western Pacific Ocean. The aim of this study was to assess the influence of this seamount on the distribution of virioplankton.

## 2 | MATERIALS AND METHODS

### 2.1 | Study site and sampling strategy

The Caroline Seamount (10.3–10.9°N, 139.9–140.4°E) is located in the tropical western Pacific Ocean. With a summit depth of 57 m, it is a typical shallow seamount. Its summit has a "basin" with a depth of ~100 m. Seawater samples were collected at the Caroline Seamount on the WPOS-M4 cruise conducted from August 7–September 5, 2017, aboard the R/V "*Kexue*." Twenty-two stations were sampled along Transects A and B crossing at Stn. 0 (Figure 1 and Table A2). To evaluate the influences of the seamount on virioplankton distribution, sampling stations were divided into two categories: stations with depths <2,000 m (except for Stn. 4, remote from the seamount) were designated as seamount stations (Stns. 0–3, 5–6, 11–12, and 17–18); while others located at >2,000 m (Stns. 7–10, 13–16, and 19–21; Stn. 4 (1,521 m)) were designated as far-field stations outside the Caroline Seamount. Stations 0, 1, and 5 were at the summit of the seamount. At each station, seawater samples were collected in 10-L Niskin bottles from the surface to the benthic-boundary layer at 4–13 different depths (Table A1). At the seamount summit, samples were also taken at the benthic-boundary layer ~5–16 m above the sediments. Conductivity-derived salinity, temperature, and pressure (sampling depth) were measured with the SBE 9 conductivity–temperature–depth profiler (Sea-Bird). In situ chlorophyll *a* (Chl *a*) fluorescence was measured with a fluorometer and turbidity sensor (FLNTU; WET

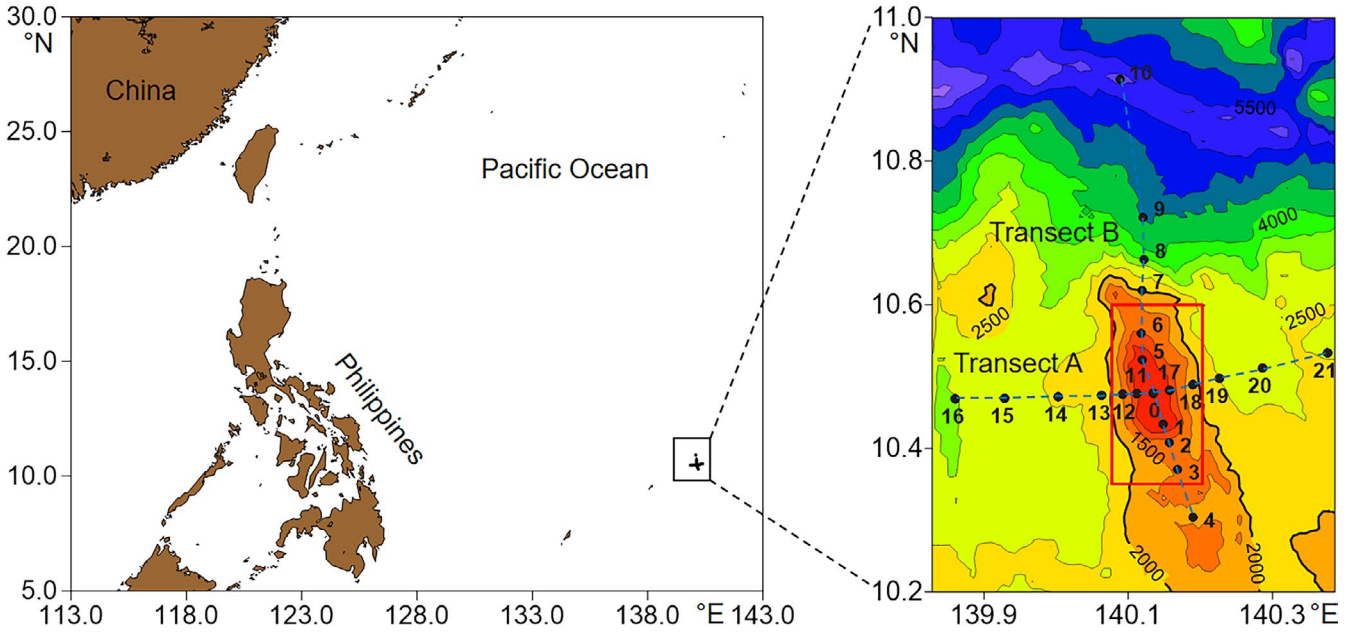



**FIGURE 1** Sampling stations in the Caroline Seamount. Stations inside the red rectangle are seamount stations. Others are far-field stations. Contours are depths in meters. Figures created with Golden Software Surfer v. 13 https://www.goldensoftware.com/products/surfer

Labs, Inc.) mounted on the sampling rosette frame. The accuracies of the conductivity, temperature, and pressure are 0.0003 S/m, 0.001°C, and 0.015% FS, respectively.

## 2.2 | Sample analysis

For virioplankton and picoplankton enumeration, 4-ml seawater samples were fixed immediately after collection with 1% (v/v) paraformaldehyde for 30 min in the dark at room temperature, flash-frozen in liquid nitrogen, and stored at −80°C until analysis in the onshore laboratory (Marie, Brussaard, Thyrhaug, Bratbak, & Vaulot, 1999; Marie, Partensky, Vaulot, & Brussaard, 1999).

Virioplankton were carried out as described by Brussaard, Payet, Winter, and Weinbauer (2010) with some modifications. Fixed samples were thawed in the dark at room temperature and filtered through a 100-µm mesh to remove large particles. The filtered samples were 10-fold diluted in 0.22-µm filtered, autoclaved TE buffer (Tris-EDTA, 100 mM Tris-Cl, 10 mM EDTA, pH 8.0; Sigma). SYBR Green I commercial stock (10,000×) was 100-fold diluted into distilled water to prepare a working solution. The samples were stained with the SYBR Green I working solution at a final $5 \times 10^{-5}$ commercial stock dilution, incubated for 10 min in the dark at 80°C, and cooled for 5 min before analysis. VLP were determined with a CytoFLEX flow cytometer (Beckman Coulter) fitted with violet (405 nm), blue (488 nm), and red (638 nm) lasers. The trigger was set to green fluorescence. Several VLP subclusters were identified on the basis of the violet side scatter versus the SYBR Green I green fluorescence intensities. The total VLP was the sum of all viral subcluster abundances.

Picoplanktonic constituents such as the photosynthetic *Synechococcus* (SYN), *Prochlorococcus* (PRO), picoeukaryotes (PEUK), and heterotrophic prokaryotes (HP) were determined with a FACSJazz flow cytometer (Becton Dickinson). The protocols were adapted from Marie, Simon, Guillou, Partensky, and Vaulot (2000). Fluorescent polystyrene beads (2 µm; Polysciences) were used as the internal standard. Autotrophic picoplankton (SYN, PRO, and PEUK) were distinguished according to their scatter and autofluorescence induced by chlorophyll *a* and/or phycoerythrin. For HP, the samples were diluted 6 folds with TE buffer and stained with SYBR Green I at a final concentration of $10^{-4}$ of the commercial stock for 20 min in the dark at room temperature. The HP were then resolved according to their fluorescence indicated on the green fluorescence versus side scatter cytogram.

Aliquots of 250-ml seawater were passed through 0.7-µm GF/F glass fiber filters (Whatman) to determine nutrient concentrations. The filtrates were fixed with trichloromethane (chloroform; $CHCl_3$) ($2 \times 10^3$, v/v) and stored in high-density polyethylene (HDPE) bottles at −20°C until analysis. The $NH_4^+$, $NO_2^-$, $NO_3^-$, and $PO_4^{3-}$ concentrations were photometrically determined in a continuous flow analyzer (QuAAtro, Bran-Luebbe Inc.).

## 2.3 | Data and statistical analyses

Virioplankton data were collected and analyzed in CytExpert v. 2.3.0.84 (Beckman Coulter). Picoplankton data were collected with BD FACS™ Software v. 1.2.0.87 (Becton Dickinson) and analyzed with the Summit v. 4.3 (Dako Colorado, Inc.). The depth-averaged integrated virioplankton and picoplankton abundances in

the epipelagic layers (0–200 m) were calculated by the trapezoidal method. Contour plots were generated with Surfer v. 13 (Golden Software). Independent *t* test and ANOVA were conducted in SPSS v. 17 (SPSS Inc.) to compare the picoplankton and virioplankton abundances between the seamount and far-field stations in the upper 75 m water column and the virioplankton/prokaryote ratios (VPR) at various depths, respectively. To elucidate the relationships among the virioplankton, picoplankton, and environmental factors, a redundancy analysis (RDA) was performed in CANOCO for Windows v. 4.5 (Microcomputer Power). A distance-based multivariate analysis for a linear model using forward selection (DISTLM forward) was run in Primer v. 6 with the PERMANOVA + package (Primer-E; Plymouth, UK) to evaluate the relative influences of factors potentially controlling virioplankton abundance (temperature, salinity, depth, in situ Chl *a* fluorescence, nutrient levels, and other picoplankton components). Where necessary, the data were logarithmically (base 10) transformed to achieve variance homogeneity and meet the normality assumptions for the regression and redundancy analyses.

## 3 | RESULTS

### 3.1 | Hydrological and biological variables

In the epipelagic layers of most Caroline Seamount stations, the current flowed from east to west at an average velocity of ~200 mm/s (J. Ma & X. Li, unpublished data). The seawater temperature ranged from 1.62°C (Stn. 16; 2,730 m depth) to 31.00°C (Stn. 5; 3 m depth). The average surface temperature was 30.48 ± 0.23°C ($n$ = 22). Temperature decreased with depth and there was a thermocline at 100–200 m (Figure 2c,d). The salinity range was 33.00–35.13, and a halocline was observed at 100–200 m (Figure 2g,h). The isotherms and isohalines decreased over the summit (Figure 2c,d,g).

There were no obvious $NO_2^-$ and $NH_4^+$ distribution trends throughout the water column. However, the higher $NH_4^+$ concentrations were observed on the east (Figure 2i,k) and north (Figure 2j,l) sides of the Caroline Seamount. Higher $NO_2^-$ concentrations were found on the east side of the Caroline Seamount (Figure 2m,o). The $NO_3^-$ and $PO_4^{3-}$ distribution patterns were similar. Their concentrations were lower in the epipelagic than the mesopelagic (200–1,000 m) and bathypelagic (1,000–3,000 m) layers (Figure 2q–x). Clear $NO_3^-$ and $PO_4^{3-}$ uplifts were observed near the summit (Figure 2s,w).

The in situ Chl *a* fluorescence was comparatively higher in the 75–200 m water column. A deep chlorophyll maximum (DCM) was located at around 100–150 m depth (Figure 3c,d). Picoplankton were distributed mainly in the epipelagic layers but decreased sharply in the mesopelagic and bathypelagic layers. PRO dominated the autotrophic picoplankton with an average abundance of 20.35 ± 31.40 × $10^3$ cells/ml, which was about two orders of magnitude higher than SYN (0.61 ± 0.38 × $10^3$ cells/ml) and PEUK (0.82 ± 0.51 × $10^3$ cells/ml) (Table 1). HP was the most abundant picoplankton with an average abundance of 4.97 ± 1.79 × $10^5$ cells/ml. Vertical distribution patterns of picoplankton were different. PRO and PEUK showed similar patterns with high abundance around the DCM layer but the maximum depth for PEUK (100–150 m) was slightly deeper than that of PRO (75–150 m). The abundance of SYN showed a maximum at 0–100 m which was above the DCM layer. High HP abundance was detected in the epipelagic layers and its maximum occurred above the DCM (Figure 3s,t).

### 3.2 | Viral subclusters

Several distinct viral subclusters could be distinguished on the cytograms of violet side scatter against SYBR Green I green fluorescence intensities (Figure A1). In the samples collected from 0 to 75 m water column, there were four distinct subclusters classified as low fluorescence viruses (LFV), medium fluorescence viruses a and b (MFV-a and MFV-b), and high fluorescence viruses (HFV) (Figure A1a,b). In the DCM deep layer samples, only a single medium fluorescence (MFV) subcluster was resolved (Figure A1c,d).

Low fluorescence viruses was the most abundant (0.25–11.86 × $10^6$ particles/ml; average 2.45 ± 1.62 × $10^6$ particles/ml) followed by MFV (0.15–8.10 × $10^6$ particles/ml; average 2.36 ± 1.90 × $10^6$ particles/ml) (Table 1; Figure A1e). HFV was least abundant subcluster (Table 1; Figure A1e). Its range was 0.01–2.14 × $10^6$ particles/ml, and its average was 0.56 ± 0.54 × $10^6$ particles/ml.

### 3.3 | Virioplankton distribution

#### 3.3.1 | Virioplankton abundance

The total VLP abundance in the Caroline Seamount was in the range of 0.64 × $10^6$–18.77 × $10^6$ particles/ml with an average of 5.37 ± 3.75 × $10^6$ particles/ml (Table 1). Similar to the various picoplankton clusters, VLP was also relatively more abundant in the epipelagic layers. Its maximum abundance was measured in 50–150 m at most stations (Figure 4c,d). The average total VLP abundance decreased from 7.23 ± 3.21 × $10^6$ particles/ml in the epipelagic layers to 1.30 ± 0.49 × $10^6$ particles/ml in the bathypelagic layers. We identified uplifted VLP abundance isolines over the summit, especially on the south side (Figure 4d). In the mesopelagic and bathypelagic layers, the total VLP abundance was higher on the east side than the west side of the Caroline Seamount (Figure 4a).

Low fluorescence viruses abundance peaked in the upper 150 m water column. This pattern roughly corresponded to those for the SYN and HP maxima (Figure 4g,h). Comparatively higher LFV abundance was observed on the east side of the Caroline Seamount (Figure 4e,g). Both MFV and HFV presented with maximum abundances at 50–150 m depth. This trend aligned with the observed PRO and PEUK distribution patterns (Figure 4k,l,o,p). All three viral

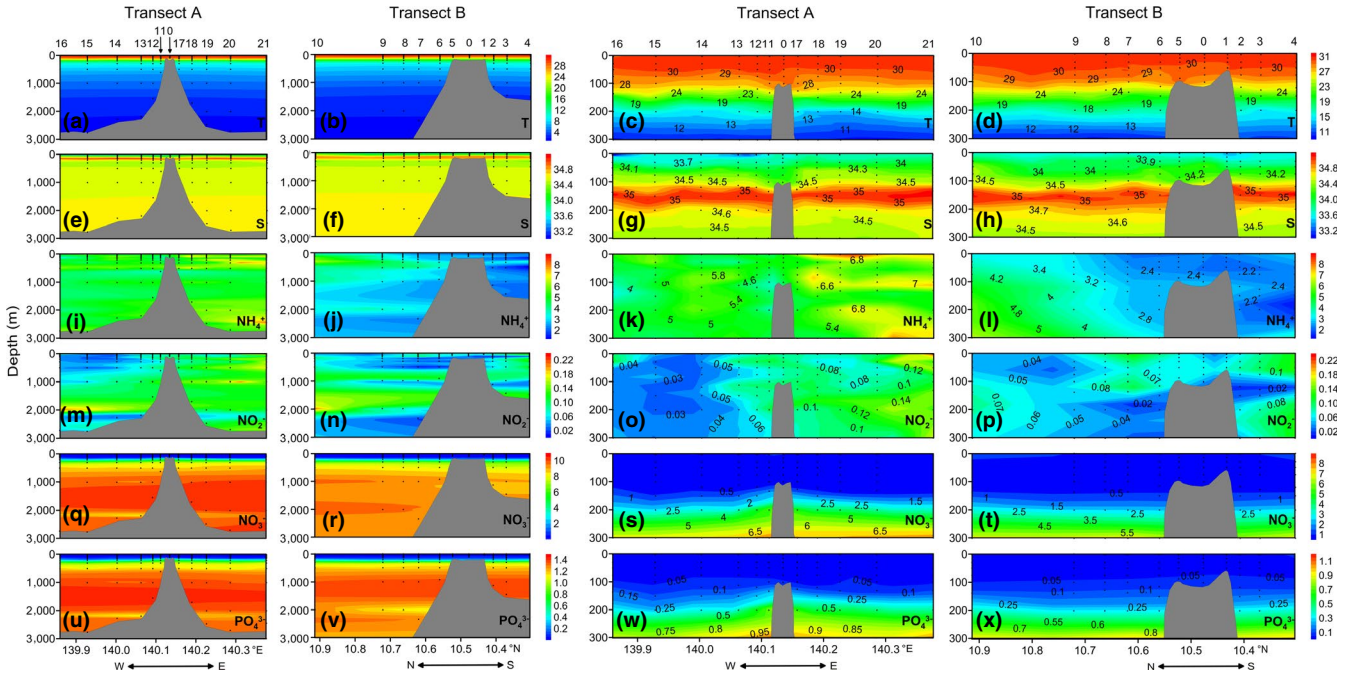



**FIGURE 2** Vertical distributions of environmental factors along Transects A and B in 0–3,000 m (1st and 2nd columns) and 0–300 m (3rd and 4th columns) water columns in the Caroline Seamount. T (a-d): temperature, °C; S (e-h): salinity; $NH_4^+$ (i-l), $NO_2^-$ (m-p), $NO_3^-$ (q-t), $PO_4^{3-}$ (u-x): μmol/L. E, east; N, north; S, south; W, west. Figures created in Golden Software Surfer v. 13, https://www.goldensoftware.com/products/surfer

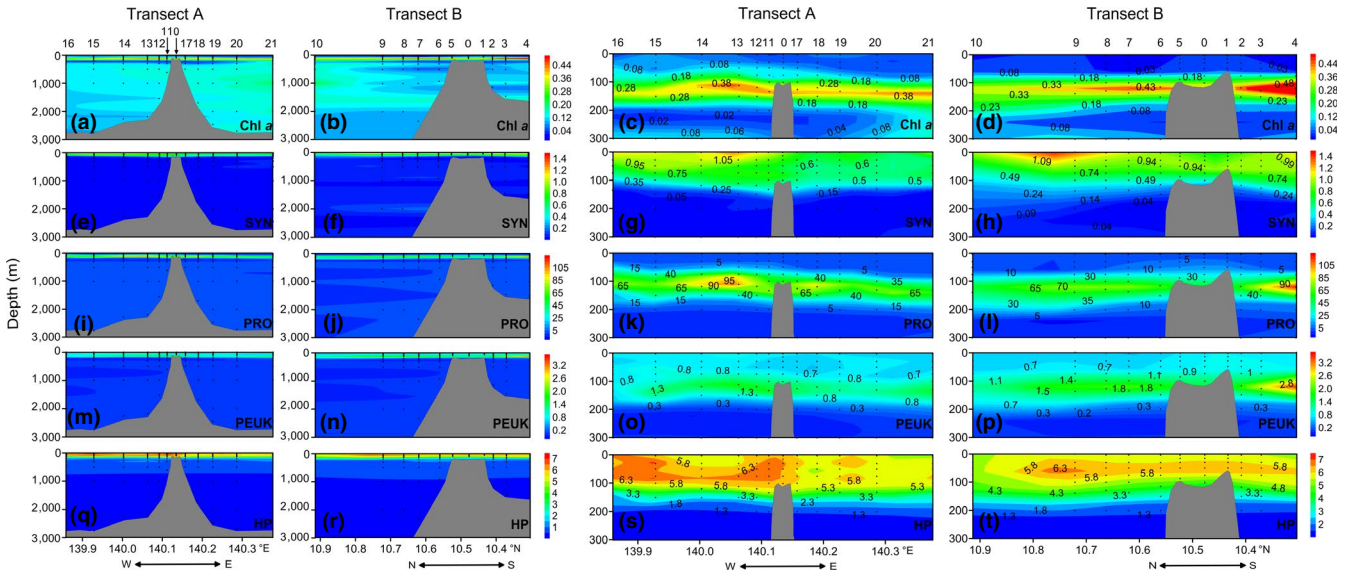



**FIGURE 3** Vertical distributions of in situ Chl *a* fluorescence and picoplankton abundance along Transects A and B in 0–3,000 m (1st and 2nd columns) and 0–300 m (3rd and 4th columns) water columns in the Caroline Seamount. Chl *a* (a-d): in situ Chl *a* fluorescence; SYN (e-h): Synechococcus , ×$10^3$ cells/ml; PRO (i-l): Prochlorococcus , ×$10^3$ cells/ml; PEUK (m-p): picoeukaryotes, ×$10^3$ cells/ml; HP (q-t): heterotrophic prokaryotes, ×$10^5$ cells/ml. E, east; N, north; S, south; W, west. Figures created in Golden Software Surfer v. 13 https://www.goldensoftware.com/products/surfer

subclusters had uplifted isolines over the summit. LFV contributed the most to the total VLP especially in the mesopelagic and bathypelagic layers (Figures A1f and 4e,f). In the 75–150 m water column, however, the abundance of MFV surpassed that of LFV (Figures A1f and 4k,l). HFV was the least abundant subcluster and comprised only 1.39%–13.13% of the total VLP (Figure A1f).

In the Caroline Seamount, the range of VPR was 4.41–83.16 throughout the water column and its average was 21.71 ± 13.64 ($n$ = 218; Table 1). VPR significantly increased with depth (15.88 ± 6.61 in the epipelagic layers, 25.99 ± 10.92 in the mesopelagic layers, and 45.49 ± 15.32 in the bathypelagic layers) at all sampling stations (one-way ANOVA; $p < .01$).

**TABLE 1** Environmental factors and picoplankton and virioplankton abundances in the Caroline Seamount

| | Epipelagic (0–200 m) | Mesopelagic (200–1,000 m) | Bathypelagic (1,000–3,000 m) | Water column (0–3,000 m) |
|---|---|---|---|---|
| Temperature (°C) | 27.01 ± 4.93 | 9.77 ± 4.12 | 3.33 ± 1.33 | 20.07 ± 10.77 |
| Salinity | 34.25 ± 0.48 | 34.54 ± 0.10 | 34.60 ± 0.05 | 34.35 ± 0.41 |
| In situ Chl *a* fluorescence | 0.13 ± 0.16 | 0.10 ± 0.05 | 0.12 ± 0.04 | 0.12 ± 0.13 |
| $NO_2^-$ (μmol/L) | 0.07 ± 0.05 | 0.08 ± 0.05 | 0.10 ± 0.06 | 0.07 ± 0.05 |
| $NO_3^-$ (μmol/L) | 0.50 ± 0.94 | 6.70 ± 2.76 | 9.71 ± 0.55 | 3.19 ± 3.97 |
| $NH_4^+$ (μmol/L) | 4.22 ± 1.80 | 4.52 ± 1.58 | 4.42 ± 1.48 | 4.33 ± 1.73 |
| $PO_4^{3-}$ (μmol/L) | 0.09 ± 0.14 | 0.95 ± 0.38 | 1.34 ± 0.08 | 0.46 ± 0.54 |
| SYN (×$10^3$ cells/ml) | 0.61 ± 0.38 | 0.04 ± 0.04 | 0.04 ± 0.03 | 0.42 ± 0.41 |
| PRO (×$10^3$ cells/ml) | 20.35 ± 31.40 | 0.78 ± 1.64 | 0.16 ± 0.08 | 13.62 ± 27.32 |
| PEUK (×$10^3$ cells/ml) | 0.82 ± 0.51 | 0.04 ± 0.08 | 0.01 ± 0.01 | 0.55 ± 0.57 |
| HP (×$10^5$ cells/ml) | 4.97 ± 1.79 | 0.86 ± 0.36 | 0.29 ± 0.07 | 3.50 ± 2.54 |
| VLP (×$10^6$ particles/ml) | 7.23 ± 3.21 | 2.06 ± 0.98 | 1.30 ± 0.49 | 5.37 ± 3.75 |
| LFV (×$10^6$ particles/ml) | 3.12 ± 1.56 | 1.24 ± 0.63 | 1.02 ± 0.48 | 2.45 ± 1.62 |
| MFV (×$10^6$ particles/ml) | 3.29 ± 1.64 | 0.73 ± 0.42 | 0.26 ± 0.06 | 2.36 ± 1.90 |
| HFV (×$10^6$ particles/ml) | 0.81 ± 0.50 | 0.10 ± 0.08 | 0.03 ± 0.01 | 0.56 ± 0.54 |
| VPR | 15.88 ± 6.61 | 25.99 ± 10.92 | 45.49 ± 15.32 | 21.71 ± 13.64 |

Abbreviations: HFV, high fluorescence viruses; HP, heterotrophic prokaryotes; LFV, low fluorescence viruses; MFV, medium fluorescence viruses; PEUK, picoeukaryotes; PRO, *Prochlorococcus*; SYN, *Synechococcus*; VLP, virus-like particles; VPR, virioplankton/prokaryote ratio.

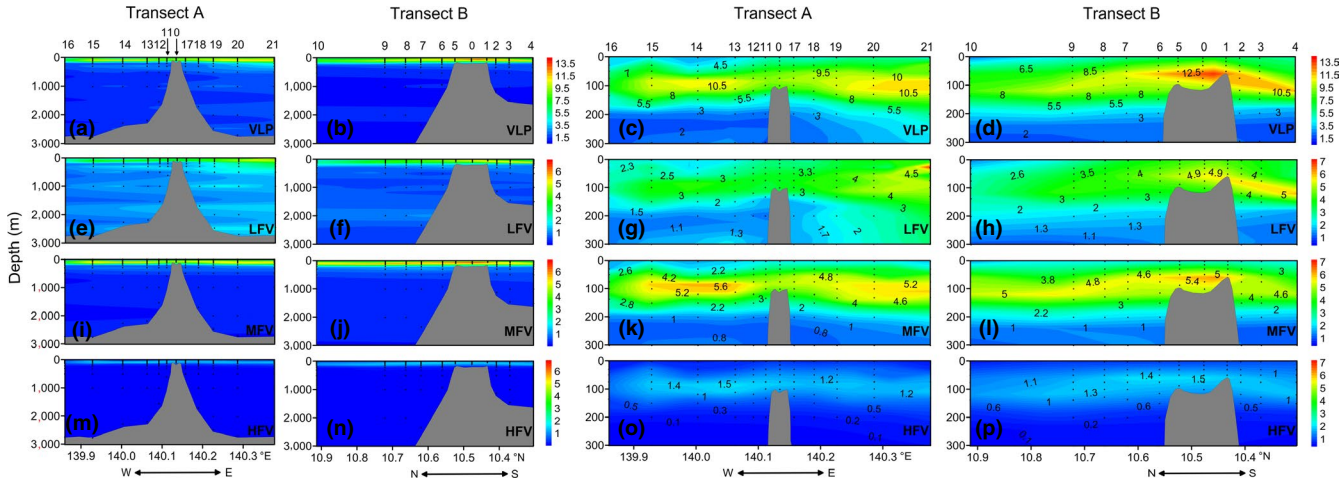



**FIGURE 4** Vertical virioplankton abundance distributions along Transects A and B in 0–3,000 m (1st and 2nd columns) and 0–300 m (3rd and 4th columns) water columns in the Caroline Seamount. VLP (a-d): virus-like particles, ×$10^6$ particles/ml; LFV (e-h): low-fluorescence viruses, ×$10^6$ particles/ml; MFV (i-l): medium-fluorescence viruses, ×$10^6$ particles/ml; HFV (m-p): high-fluorescence viruses, ×$10^6$ particles/ml. E, east; N, north; S, south; W, west. Figures created in Golden Software Surfer v. 13 https://www.goldensoftware.com/products/surfer

### 3.3.2 | Virioplankton in the seamount and far-field stations

The vertical and horizontal distribution patterns of the virioplankton differed between the seamount and far-field stations. At the seamount stations, the total VLP and all three viral subclusters presented with subsurface maxima at 75 m depth (Figure A2a,c,e,g). At the far-field stations, the total VLP, MFV, and HFV showed DCM maxima at 100 m. LFV had a DCM peak at 125 m. However, there were no observable vertical differences in picoplankton distribution between the seamount and far-field stations (Figure A2i–p).

The total VLP and all three viral subclusters had similar horizontal distribution patterns in the Caroline Seamount based on the depth-averaged integrated abundance in the epipelagic layers (Figure 5). Maximum VLP, LFV, MFV, and HFV abundances were measured around the seamount summit. The abundances decreased from the seamount stations to the far-field stations (Figures 5 and A3). Significantly higher VLP, LFV, and HFV abundances were noted at the seamount stations than the far-field stations in the upper 75 m water column ($n$ = 88; independent $t$ test; $p < .01$, $p < .01$, and $p < .05$, respectively) (Table 2). The MFV abundance was also higher at the seamount stations than the far-field stations but the difference was not

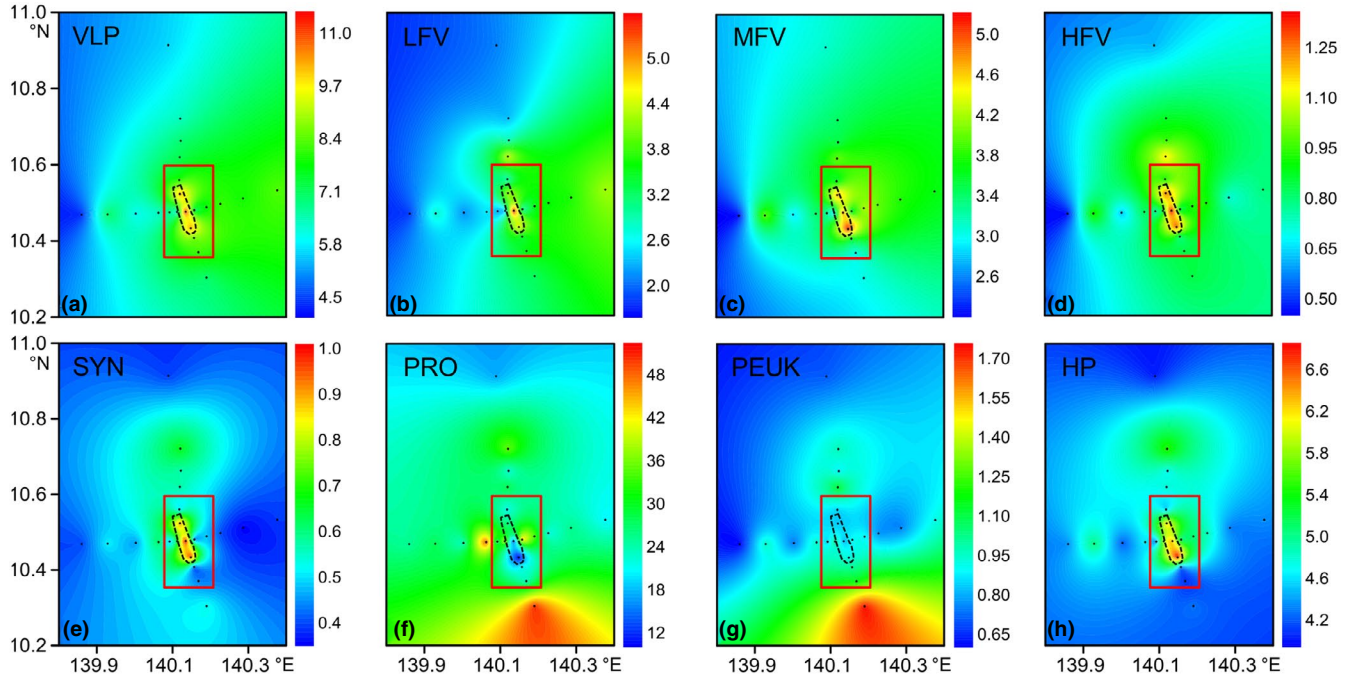



**FIGURE 5** Horizontal distributions of depth-averaged integrated virioplankton and picoplankton abundances in the epipelagic layers. Black dotted lines indicate the location of Caroline Seamount summit. Seamount stations are inside the red rectangle. Others are far-field stations. VLP (a): virus-like particles, $\times 10^6$ particles/ml; LFV (b): low-fluorescence viruses, $\times 10^6$ particles/ml; MFV (c): medium-fluorescence viruses, $\times 10^6$ particles/ml; HFV (d): highfluorescence viruses, $\times 10^6$ particles/ml. SYN (e): Synechococcus , $\times 10^3$ cells/ml; PRO ( f ) : Prochlorococcus , $\times 10^3$ cells/ml; PEUK (g): picoeukaryotes, $\times 10^3$ cells/ml; HP (h): heterotrophic prokaryotes, $\times 10^5$ cells/ml. Figures created in Golden Software Surfer v. 13 https://www.goldensoftware.com/products/surfer

**TABLE 2** Virioplankton and picoplankton abundances in seamount and far-field stations in the upper 75 m water column

| | Seamount stations ($n$ = 41) | Far-field stations ($n$ = 47) | $t$ test significance |
|---|---|---|---|
| VLP ($\times 10^6$ particles/ml) | 8.31 ± 2.87 | 6.50 ± 2.68 | ** |
| LFV ($\times 10^6$ particles/ml) | 3.82 ± 1.41 | 2.87 ± 1.29 | ** |
| MFV ($\times 10^6$ particles/ml) | 3.57 ± 1.64 | 2.90 ± 1.42 | NS |
| HFV ($\times 10^6$ particles/ml) | 0.92 ± 0.48 | 0.72 ± 0.42 | * |
| SYN ($\times 10^3$ cells/ml) | 0.83 ± 0.18 | 0.85 ± 0.23 | NS |
| PRO ($\times 10^3$ cells/ml) | 7.36 ± 13.72 | 6.34 ± 14.68 | NS |
| PEUK ($\times 10^3$ cells/ml) | 0.73 ± 0.13 | 0.73 ± 0.09 | NS |
| HP ($\times 10^5$ cells/ml) | 5.88 ± 0.48 | 5.89 ± 0.58 | NS |
| VPR | 14.17 ± 4.88 | 11.08 ± 4.61 | ** |

*Note: t* test; NS, not significant.

Abbreviations: HFV, high fluorescence viruses; HP, heterotrophic prokaryotes; LFV, low fluorescence viruses; MFV, medium fluorescence viruses; PEUK, picoeukaryotes; PRO, *Prochlorococcus*; SYN, *Synechococcus*; VLP, virus-like particles; VPR, virioplankton/prokaryote ratio.

*$p < .05$.

**$p < .01$.

significant ($p > .05$). The VPR was significantly higher at the seamount stations than the far-field stations ($p < .01$; Table 2). The SYN and HP abundances exhibited horizontal trends similar to those for the virioplankton with higher abundance at seamount stations, while PRO and PEUK abundances displayed no clear horizontal pattern (Figure 5). No significant difference in picoplankton abundance was identified between the seamount and far-field stations ($p > .05$; Table 2).

### 3.4 | Factors influencing virioplankton

A redundancy analysis (RDA) was performed to assess the relationships among the virioplankton, picoplankton, and environmental factors (Figure 6). The first two axes explained 78.4% of the total inertia in the virioplankton abundance and 96.1% of the cumulative variance of virioplankton, picoplankton, and environmental factor

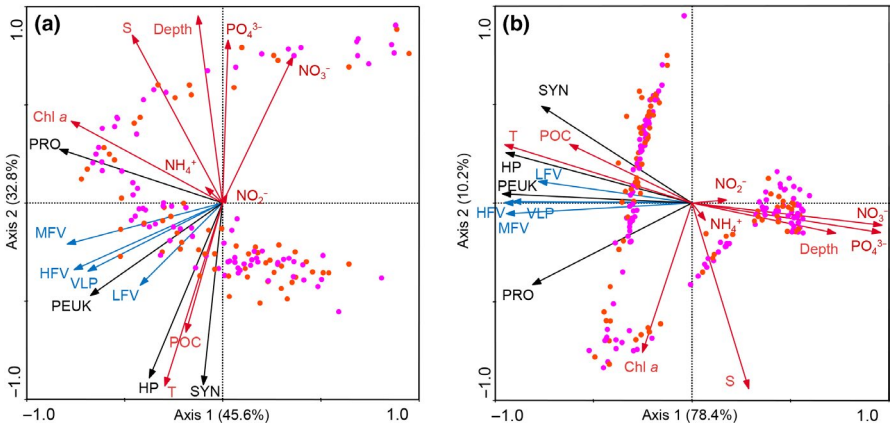



**FIGURE 6** Redundancy analysis (RDA) of virioplankton and picoplankton abundances and environmental factors in the epipelagic layers (a) and entire water column (b). Blue arrows: virioplankton; black arrows: picoplankton; red arrows: environmental factors. Orange dots: seamount stations; pink dots: far-field stations. Chl *a*, in situ Chl *a* fluorescence; HFV, high fluorescence viruses; HP, heterotrophic prokaryotes; LFV, low fluorescence viruses; MFV, medium fluorescence viruses; PEUK, picoeukaryotes; POC, particulate organic carbon; PRO, *Prochlorococcus*; S, salinity; SYN, *Synechococcus*; T, temperature; VLP, virus-like particles. Figures created in Microcomputer Power CANOCO for Windows v. 4.5 http://www.microcomputerpower.com/

relationships in the epipelagic layers (Figure 6a). The total VLP had a positive relationship with PEUK abundance, and a negative relationship with nutrients especially $NO_3^-$ and $PO_4^{3-}$. The RDA disclosed a very strong positive relationship between LFV and HP as well as PEUK. MFV and HFV were also positively correlated with PEUK but only moderately positively correlated with PRO and SYN. All viral groups were weakly positively correlated with in situ Chl *a* fluorescence and particulate organic carbon (POC) (Ma et al., unpublished data). The correlations for the entire water column resembled those for the epipelagic layers (Figure 6b).

A distance-based multivariate analysis for a linear model using forward selection (DISTLM forward) was performed as an attempt to explain the variation of virioplankton abundance between seamount stations and far-field stations (Table 3). At the far-field stations, the abundance of potential hosts, especially PRO and HP, as well as temperature and nitrate were main variables that explained the variation of virioplankton. For the seamount stations, however, environmental factors such as water temperature and nitrate concentration rather than host abundance were the factors that most significantly influenced virioplankton distribution there (Table 3).

## 4 | DISCUSSION

The present study elaborated virioplankton distribution in the Caroline Seamount of the tropical western Pacific Ocean. Virioplankton abundance in the water column was comparable with those reported for previous studies conducted in the Pacific Ocean (Brum, 2005; Hwang & Cho, 2010; Li et al., 2014; Liang et al., 2017; Rowe et al., 2012; Yang, Motegi, Yokokawa, & Nagata, 2010; Yang, Yokokawa, Motegi, & Nagata, 2014) and other pelagic oceans (De Corte et al., 2010, 2012; Evans, Pearce, & Brussaard, 2009; Lara et al., 2017).

### 4.1 | Viral subclusters

Using flow cytometry, the viral community could be divided into several subclusters with different green fluorescence intensities and side scatter signature (Brussaard et al., 2010). In natural samples, two to five viral subclusters were identified from distinct aquatic ecosystems (Baudoux, Veldhuis, Noordeloos, Noort, & Brussaard, 2008; Brussaard, Timmermans, Uitz, & Veldhuis, 2008; Liang et al., 2014; Mojica, Huisman, Wilhelm, & Brussaard, 2016). However, most studies found only two or three viral subclusters (Table 4). Here, we identified three to four subclusters with similar side scatter but different green fluorescence intensities.

Although no significant linear correlation between genome size and SYBR Green I fluorescence intensities of viral subclusters was found, different fluorescence intensities may partially reflect genome size variations (Brussaard et al., 2010). Phages infecting heterotrophic prokaryotes usually have small genomes size and low nucleic acid green fluorescence in FCM analysis (Brussaard, Marie, & Bratbak, 2000; Larsen et al., 2001). LFV consist mainly of small phages infecting heterotrophic prokaryotes (Larsen et al., 2004; Marie, Brussaard, et al., 1999). In natural samples, LFV abundance often covaries with that of HP (Mojica et al., 2016; Payet, McMinds, Burkepile, & Vega Thurber, 2014). Our redundancy analysis also corroborated this pattern. Mojica et al. (2016) described correlations between MFV and PEUK and between HFV and picocyanobacteria across the north Atlantic Ocean. Yang et al. (2010) reported a correlation between HFV and picophytoplankton (including SYN, PRO, and PEUK) in the Pacific Ocean. Our results showed that in the tropical western Pacific Ocean, the abundances of MFV and HFV were strongly positively correlated with PEUK and, to a lesser extent, with SYN and PRO (Figure 6), indicating that the MFV and HFV subclusters contain cyanophages and algal viruses. Pulsed-field gel electrophoresis (PFGE) and sorting-combined sequencing identified cyanophage and eukaryotic algal viral sequences in the MFV

**TABLE 3** Multivariate regression analyses with forward selection (DISTLM forward) explaining variabilities in virioplankton and picoplankton abundances and environmental factors in the epipelagic layers of Caroline Seamount

| | Selected variables | Pseudo-F | *P* | $r^2$ | Cumulative |
|---|---|---|---|---|---|
| Seamount stations (*n* = 63) | | | | | |
| VLP | $NO_3^-$ | 54.69 | 0.001 | 0.47 | 0.47 |
| | S | 19.01 | 0.001 | 0.10 | 0.57 |
| | PRO | 6.85 | 0.011 | 0.05 | 0.62 |
| | HP | 6.45 | 0.011 | 0.05 | 0.67 |
| LFV | T | 56.87 | 0.001 | 0.48 | 0.48 |
| | $NO_3^-$ | 9.04 | 0.009 | 0.07 | 0.55 |
| MFV | $NO_3^-$ | 37.50 | 0.001 | 0.38 | 0.38 |
| | HP | 56.35 | 0.001 | 0.23 | 0.61 |
| | S | 17.20 | 0.001 | 0.14 | 0.75 |
| | PRO | 10.79 | 0.006 | 0.04 | 0.79 |
| HFV | $NO_3^-$ | 40.40 | 0.001 | 0.40 | 0.40 |
| | S | 77.28 | 0.001 | 0.24 | 0.64 |
| | PRO | 12.52 | 0.001 | 0.10 | 0.74 |
| | HP | 10.16 | 0.003 | 0.07 | 0.81 |
| Far-field stations (*n* = 83) | | | | | |
| VLP | T | 64.73 | 0.001 | 0.32 | 0.32 |
| | S | 30.92 | 0.001 | 0.28 | 0.60 |
| LFV | HP | 20.31 | 0.001 | 0.20 | 0.20 |
| | S | 22.24 | 0.001 | 0.17 | 0.37 |
| | $NO_2^-$ | 8.22 | 0.005 | 0.06 | 0.43 |
| MFV | PRO | 42.03 | 0.001 | 0.34 | 0.34 |
| | $NO_3^-$ | 30.91 | 0.001 | 0.18 | 0.52 |
| | T | 54.34 | 0.001 | 0.14 | 0.66 |
| | Depth | 28.96 | 0.001 | 0.13 | 0.79 |
| HFV | $NO_3^-$ | 50.99 | 0.001 | 0.39 | 0.39 |
| | Depth | 41.28 | 0.001 | 0.21 | 0.60 |
| | T | 57.20 | 0.001 | 0.17 | 0.77 |
| | HP | 13.51 | 0.001 | 0.03 | 0.80 |

*Note:* The response variable was log-transformed and resulting data converted into Euclidian distance similarity matrices. Pseudo-F and *P* values obtained by permutation (*n* = 999).

Abbreviations: HFV, high fluorescence viruses; HP, heterotrophic prokaryotes; LFV, low fluorescence viruses; MFV, medium fluorescence viruses; PRO, *Prochlorococcus*; S, salinity; T, temperature; VLP, virus-like particles.

and HFV subclusters (Larsen, Larsen, Thyrhaug, Bratbak, & Sandaa, 2008; Martínez, Swan, & Wilson, 2014).

Here, we discovered that the dominant viral subcluster varied with depths. LFV dominated in the mesopelagic and bathypelagic layers whereas MFV exceeded LFV to be the most abundant subcluster in the midepipelagic layer (75–150 m). In contrast, previous studies reported no variation of the dominant viral subclusters. HFV was least abundant subcluster and its abundance decreased with depth. Similar results were reported for studies conducted in the South Atlantic Ocean (De Corte, Sintes, Yokokawa, Lekunberri, & Herndl, 2016). Most studies demonstrated a clear LFV dominance throughout the water column (Wei, Zhang, Peng, Liang, & Jiao, 2018; Winter et al., 2009; Yang et al., 2010). Magiopoulos and Pitta (2012) indicated that in the Eastern Mediterranean Sea, LFV were the dominant viral group, but the dominance was lower in the mesopelagic layer compared to the epipelagic and bathypelagic layers. However, De Corte et al. found the most abundant viral subcluster was MFV throughout the water column in the Atlantic Ocean (De Corte et al., 2010, 2012). Viruses cannot replicate without host cells. Thus, viral abundance is closely associated with the abundance of their (mostly) microbial hosts. Large-scale analyses of the global tropical and subtropical oceans proved that potential host abundance is to some extent a significant influencing factor of virioplankton (Lara et al., 2017). Picophytoplankton abundance was high in the vicinity of the DCM layer but sharply decreased below it. In the mesopelagic and bathypelagic layers, the abundance of HP was much higher than that of picophytoplankton (Figure 3). Therefore, the variation of host cells (picophytoplankton and HP) abundance in different depths might account for the discrepancies we observed among the layers in terms of their dominant viral subclusters.

We also noticed that viral subclusters varied with depth. The MFV-a and MFV-b subclusters were identified above DCM (0–75 m). Below DCM, however, only a single MFV subcluster was identified. In the tropical western Pacific Ocean, the cyanobacteria SYN and PRO are the major picophytoplankton contributors (Figure 3). Therefore, they are potential MFV hosts. MFV subcluster variation cooccurred with depth niche partitioning of SYN and PRO. SYN is usually restricted to the upper well-lit layers in oligotrophic areas (Partensky, Blanchot, & Vaulot, 1999). At 0–75 m where subclusters MFV-a and MFV-b were detected, SYN accounts for a significant portion of cyanobacteria abundance and the abundance of PRO was low (Figure 3). PRO can colonize in the subsurface water even with only 0.1% of the surface irradiance (Partensky et al., 1999). As the water depth increases, PRO becomes the dominant cyanobacteria, and the portion of SYN become negligible (Figure 3). Meanwhile, a single MFV subcluster takes the place. These variations in the MFV subcluster probably reflected the relative differences in the dominant cyanobacterial hosts at various depths. A similar phenomenon was also found in the Eastern Indian Ocean (Yuan Zhao, unpublished data). This was in contrast to previous studies in Pacific (Liang et al., 2017; Yang et al., 2010) or other pelagic ocean regions (De Corte et al., 2012, 2016; Liang et al., 2014; Magiopoulos & Pitta, 2012; Mojica et al., 2016), which found no viral subclusters variation in different depths.

## 4.2 | Influence of seamount

Interactions between seamounts and ocean currents might influence plankton community compositions and distributions. Mendonça et al. (2012) found that, in some cases, a "seamount

**TABLE 4** Comparison of virioplankton abundance and subclusters and VPR from relevant studies

| Study areas | Abundance ($\times 10^6$ particles/ml) | Subclusters | VPR | References |
|---|---|---|---|---|
| Tropical Western Pacific Ocean | 1.30 ± 0.49–7.23 ± 3.21 | 3–4 | 15.88 ± 6.61–45.49 ± 15.32 | Present study |
| Western Pacific Ocean | 0.8 ± 0.3–6.9 ± 3.2 | 2 | 14.6 ± 5.6–21.2 ± 9.0 | Liang et al. (2017) |
| Western Pacific Ocean | 0.68 ± 0.36–5.82 ± 2.05 | | 10.08 ± 2.41–14.68 ± 6.71 | Li et al. (2014) |
| Central Pacific Ocean and the Pacific sector of the Southern Ocean | 1.5–32 | 3 | 8.6 ± 2.4–22.2 ± 14.4 | Yang et al. (2010) |
| Global cruise (South China Sea, Indian Ocean, Atlantic Ocean, Pacific Ocean) | 1.11 ± 0.78–8.94 ± 4.69 | 2 | 16.2 ± 7.9–19.0 ± 8.2 | Liang et al. (2014) |
| North Atlantic Ocean | | 5 | | Mojica et al. (2016) |
| North Atlantic latitudinal transect | 0.58 ± 0.23–4.48 ± 2.38 | 3 | 19.2 ± 8.3–59.1 ± 18.7 | De Corte et al. (2012) |
| (Sub)tropical Atlantic Ocean | 0.43 ± 0.08–2.54 ± 1.09 | 3 | 9.51 ± 2.63–25.18 ± 4.48 | De Corte et al. (2010) |
| South Atlantic Ocean | 0.61 ± 0.31–4.66 ± 4.06 | 3 | 15.0 ± 15.7–32.9 ± 25.1 | De Corte et al. (2016) |
| Eastern Mediterranean Sea | 0.12–27 | 3 | 3.9–44.2 | Magiopoulos and Pitta (2012) |
| Northwestern Mediterranean Sea | 0.9 ± 0.3–17.4 ± 19.6 | 3 | 13.9 ± 4.0–22.2 ± 15.3 | Winter et al. (2009) |
| North Sea | 5–70 | 4 | | Baudoux et al. (2008) |
| East China Sea | 0.34–2.3 | 2 | | Yang and Jiao (2002) |
| Norwegian coastal waters | | 3 | 4.3 ± 2.4 | Bratbak et al. (2011) |

Abbreviation: VPR, virioplankton/prokaryote ratio.

effect" on the microbial community structure and biomass was observed on Seine and Sedlo seamounts. The large autotrophic microbial communities at the summit and seamount stations of Seine were enhanced in the spring. In addition, maximum picoplankton biomass was measured at the summit station and near the seamount station of Sedlo in the summer. The dominance of heterotrophs is presumably related to the trapping effect of organic matter by seamounts (Mendonça et al., 2012). Sime-Ngando, Juniper, and Vézina (1992) reported that ciliate biomass was substantially higher over the seamounts than the oceanic regions of the Cobb Seamount in the eastern subarctic Pacific Ocean. However, previous studies showed that this "seamount effect" on the plankton community did not persist (Comeau, Vézina, Bourgeois, & Juniper, 1995; Genin & Boehlert, 1985; Mouriño et al., 2005; Rowden, Dower, Schlacher, Consalvey, & Clark, 2010). Not all plankton groups were affected by seamounts. The influence of seamounts on the plankton community varied with season. The data reported for different surveys on the same seamount are inconsistent. Three surveys were conducted on the Minami-Kasuga seamount but only the first detected and reported cold dome, chlorophyll increase, and high zooplankton biomass above the seamount (Genin & Boehlert, 1985).

At present, little is known about the influences of seamounts on virioplankton. In the only known study on virioplankton distributions in seamounts, Chiang and Quiñones (2007) stated that comparatively elevated viral and HP abundances were detected in the benthic-boundary layer over the Bajo O'Higgins 1 seamount summit. However, taking the depth differences between summit (376 m) and other stations (437–841 m) into account, the higher VLP abundance might not be completely attributed to the influence of seamount. Another study investigated viral abundance and production in the seamount and far-field sediments (3,000 m) of the Tyrrhenian Sea (Danovaro et al., 2009). Seamount sediments had a significantly higher virus and HP abundance than the far-field sediments. Benthic viral production in the seamount sediments was about twice that in the far-field sediments. These results suggest that seamounts significantly altered prokaryote–virus interactions in the sediments (Danovaro et al., 2009). However, the influence of seamounts on the viral abundance in the water column remains obscure.

Previous studies on the tropical western Pacific Ocean investigated the influence of seamounts on phytoplankton and microbial food web components. However, Chl *a* concentration, primary productivity, and microbial food web component abundances were not substantially enhanced over the summits of the Y3 and M2 seamounts of the western Pacific Ocean (Dai, Sun, Liang, Tian, & Liu, 2017; Zhang, Sun, Chen, Li, & Du, 2016; Zhao et al., 2017). To the best of our knowledge, then, there is no prior information about the influence of seamounts on the virioplankton of the western Pacific Ocean.

The Caroline Seamount is located in the tropical Western Pacific. It is mainly influenced by the westwards North Equatorial Current (NEC) in the upper water column (0–200 m) (Hu et al., 2015; Toole, Zou, & Millard, 1988). Deflection of isotherms and isohalines, as well as uplifts of $NO_3^-$ and $PO_4^{3-}$, was observed, indicating localized disturbances caused by the seamount structure. Muck et al. (2014) revealed turbulent mixing of deep water masses impacts not only the physicochemical parameters of the mixing zone but also the activity of viruses. Relatively higher virioplankton abundance and shallower virioplankton subsurface peaks were noted at the seamount stations. These phenomena were shaped primarily by localized disturbances created by the seamount structure.

Changes in environmental conditions such as temperature, salinity, and nutrients can strongly affect viral production and lysogeny

dynamics (Bettarel et al., 2011; Chiaki & Toshi, 2007; Li et al., 2014; Lymer & Vrede, 2006; Maurice, Bouvier, Wit, & Bouvier, 2013; Williamson & Paul, 2004). Viral abundance may increase with nutrient availability (Danovaro, Armeni, Corinaldesi, & Mei, 2003; Hewson, O'Neil, Fuhrman, & Dennison, 2001; Williamson, Houchin, McDaniel, & Paul, 2002). Turbulent mixing is conducive to higher viral production and abundance and virus-induced mortality in coastal waters (Paterson, Nayar, Mitchell, & Seuront, 2012; Wilhelm, Brigden, & Suttle, 2002) and deep waters (Muck et al., 2014; Winter et al., 2018). In the tropical western Pacific Ocean, warm surface layers above comparatively cooler and denser subsurface layers create and maintain a permanent thermocline that inhibits nutrient-rich upwells and results in surface waters with low primary productivity (Longhurst, 2007). Interactions between shallow seamounts and local currents vertically displace isotherms and isohalines above the seamounts. Nutrients such as $NO_3^-$ and $PO_4^{3-}$ are transported into the nutrient-limited euphotic zone. This process stimulates both viral and prokaryote production and increases viral abundance in Caroline Seamount. On the other hand, it is not understood why prokaryote and phytoplankton abundances do not rise concomitantly in the Caroline Seamount. Further studies are needed to elucidate the underlying mechanism of this phenomenon since multiple factors influence viral abundances in seamounts. The elevated viral abundance in the seamount may also be explained by the resuspension of viruses from the seamount floor. Sedimentary viral density was reported to be higher than that in the water column (Danovaro & Serresi, 2000). Viruses may readily detach from the sediment and enter the water column (Hassard et al., 2016). Dupuy et al. (2014) reported that free viruses were resuspended by weak flow through the sediment at friction velocities <2 cm/s. However, as previous studies on plankton communities have already proposed, the so-called "seamount effect" for virioplankton is probably not persistent. Thus, more systematic research is necessary.

## 5 | CONCLUSIONS

The present study in the tropical western Pacific Ocean showed three to four viral subclusters exhibited differences related to depth. Shallower subsurface peaks and significant virioplankton abundance enhancements were detected at the summit and seamount stations. Interactions between the shallow Caroline Seamount and the local current can support higher virioplankton standing stocks. To the best of our knowledge, this is the first report of the so-called "seamount effect" on virioplankton. However, detailed studies on viral abundance, production, and genomics around the seamount at high spatiotemporal resolutions are required to clarify and elaborate on the influences of seamounts on virioplankton dynamics.

### ACKNOWLEDGMENTS

This study was carried out within the framework of the WPOS (Western Pacific Ocean System: Structure, Dynamics and Consequences) program and was financially supported by Science & Technology Basic Resources Investigation Program of China (2017FY100803), National Key Research and Development Program of China (2017YFA0603204), National Natural Science Foundation of China (91751202), the CNRS-NSFC Joint Research Projects Program (NSFC 41711530149), and 2017-2019 Sino-French Cai Yuanpei Programme. We thank the captain and crew of the R/V "Kexue" for their help during the cruise.

### CONFLICT OF INTERESTS

None declared.

### AUTHOR CONTRIBUTION

Yanchu Zhao: Formal analysis (lead); Investigation (lead); Writing-original draft (equal); Writing-review & editing (equal). Yuan Zhao: Conceptualization (lead); Methodology (equal); Writing-original draft (lead); Writing-review & editing (lead). Shan Zheng: Formal analysis (supporting); Investigation (supporting); Writing-review & editing (equal). Li Zhao: Formal analysis (lead); Investigation (supporting); Writing-review & editing (equal). Xuegang Li: Formal analysis (supporting); Investigation (supporting); Writing-review & editing (equal). Wuchang Zhang: Conceptualization (supporting); Funding acquisition (equal); Supervision (supporting); Writing-review & editing (equal). Gérald Gregori: Methodology (equal); Writing-review & editing (equal). Tian Xiao: Conceptualization (lead); Funding acquisition (equal); Supervision (lead); Writing-review & editing (lead).

### ETHICS STATEMENT

None required.

### DATA AVAILABILITY STATEMENT

The data sets used and analyzed during the current study are available in the figshare repository at https://doi.org/10.6084/m9.figshare.11880768.

### ORCID

*Yuan Zhao* https://orcid.org/0000-0002-8892-2100

### REFERENCES

Baudoux, A. C., Veldhuis, M. J. W., Noordeloos, A. A. M., van Noort, G., & Brussaard, C. P. D. (2008). Estimates of virus- vs. grazing induced mortality of picophytoplankton in the North Sea during summer. *Aquatic Microbial Ecology*, *52*(1), 69–82. https://doi.org/10.3354/ame01207

Bergh, Ø., Børsheim, K. Y., Bratbak, G., & Heldal, M. (1989). High abundance of viruses found in aquatic environments. *Nature*, *340*(6233), 467–468. https://doi.org/10.1038/340467a0

Bettarel, Y., Bouvier, T., Bouvier, C., Carré, C., Desnues, A., Domaizon, I., … Sime-Ngando, T. (2011). Ecological traits of planktonic viruses and prokaryotes along a full-salinity gradient. *FEMS Microbiology Ecology*, *76*(2), 360–372. https://doi.org/10.1111/j.1574-6941.2011.01054.x

Boehlert, G. W., & Genin, A. (1987). A review of the effects of seamounts on biological processes. In B. H. Keating, P. R. Fryer, & W. Boehlert (Eds.), *Seamounts, islands, and atolls* (Vol. *43*, pp. 319–334). Washington, DC: American Geophysical Union. https://doi.org/10.1029/GM043p0319

Børsheim, K. Y., Bratbak, G., & Heldal, M. (1990). Enumeration and biomass estimation of planktonic bacteria and viruses by transmission electron microscopy. *Applied and Environmental Microbiology*, *56*(2), 352–356.

Bratbak, G., Jacquet, S., Larsen, A., Pettersson, L. H., Sazhin, A. F., & Thyrhaug, R. (2011). The plankton community in Norwegian coastal waters—Abundance, composition, spatial distribution and diel variation. *Continental Shelf Research*, *31*(14), 1500–1514. https://doi.org/10.1016/j.csr.2011.06.014

Brum, J. R. (2005). Concentration, production and turnover of viruses and dissolved DNA pools at Stn ALOHA, North Pacific Subtropical Gyre. *Aquatic Microbial Ecology*, *41*, 103–113. https://doi.org/10.3354/ame041103

Brussaard, C. P. D., Marie, D., & Bratbak, G. (2000). Flow cytometric detection of viruses. *Journal of Virological Methods*, *85*(1), 175–182. https://doi.org/10.1016/S0166-0934(99)00167-6

Brussaard, C. P. D., Payet, J. P., Winter, C., & Weinbauer, M. G. (2010). Quantification of aquatic viruses by flow cytometry. In S. W. Wilhelm, M. G. Weinbauer, & C. A. Suttle (Eds.), *Manual of aquatic viral ecology* (pp. 102–109). Waco, TX: American Society of Limnology and Oceanography. https://doi.org/10.4319/mave.2010.978-0-984559-1-0-7

Brussaard, C. P. D., Timmermans, K. R., Uitz, J., & Veldhuis, M. J. W. (2008). Virioplankton dynamics and virally induced phytoplankton lysis versus microzooplankton grazing southeast of the Kerguelen (Southern Ocean). *Deep Sea Research Part II: Topical Studies in Oceanography*, *55*(5–7), 752–765. https://doi.org/10.1016/j.dsr2.2007.12.034

Chiaki, M., & Toshi, N. (2007). Enhancement of viral production by addition of nitrogen or nitrogen plus carbon in subtropical surface waters of the South Pacific. *Aquatic Microbial Ecology*, *48*(1), 27–34. https://doi.org/10.3354/ame048027

Chiang, O. E., & Quiñones, R. A. (2007). Relationship between viral and prokaryotic abundance on the Bajo O'Higgins 1 Seamount (Humboldt Current System off Chile). *Scientia Marina*, *71*(1), 37–46. https://doi.org/10.3989/scimar.2007.71n137

Comeau, L. A., Vézina, A. F., Bourgeois, M., & Juniper, S. K. (1995). Relationship between phytoplankton production and the physical structure of the water column near Cobb Seamount, northeast Pacific. *Deep Sea Research Part I: Oceanographic Research Papers*, *42*(6), 993–1005. https://doi.org/10.1016/0967-0637(95)00050-G

Cordeiro, T. A., Brandini, F. P., Rosa, R. S., & Sassi, R. (2013). Deep chlorophyll maximum in western equatorial Atlantic-how does it interact with islands slopes and seamounts? *Marine Science*, *3*(1), 30–37. https://doi.org/10.5923/j.ms.20130301.03

Dai, S., Sun, X.-X., Liang, J.-H., Tian, Z.-Y., & Liu, T. (2017). Biomass of size-fractionated phytoplankton and primary producivity at M2 seamount in tropical West Pacific in Spring 2016. *Oceanologia Et Limnologia Sinica*, *48*(6), 1456–1464 (In Chinese with English abstract). https://doi.org/10.11693/hyhz20170900237

Danovaro, R., Armeni, M., Corinaldesi, C., & Mei, M. L. (2003). Viruses and marine pollution. *Marine Pollution Bulletin*, *46*, 301–304. https://doi.org/10.1016/S0025-326X(02)00461-7

Danovaro, R., Corinaldesi, C., Luna, G. M., Magagnini, M., Manini, E., & Pusceddu, A. (2009). Prokaryote diversity and viral production in deep-sea sediments and seamounts. *Deep Sea Research Part II: Topical Studies in Oceanography*, *56*(11), 738–747. https://doi.org/10.1016/j.dsr2.2008.10.011

Danovaro, R., Dell'Anno, A., Corinaldesi, C., Magagnini, M., Noble, R., Tamburini, C., & Weinbauer, M. (2008). Major viral impact on the functioning of benthic deep-sea ecosystems. *Nature*, *454*(7208), 1084–1087. https://doi.org/10.1038/nature07268

Danovaro, R., & Serresi, M. (2000). Viral density and virus-to-bacterium ratio in deep-sea sediments of the Eastern Mediterranean. *Applied and Environmental Microbiology*, *66*(5), 1857–1861. https://doi.org/10.1128/AEM.66.5.1857-1861.2000

De Corte, D., Sintes, E., Winter, C., Yokokawa, T., Reinthaler, T., & Herndl, G. J. (2010). Links between viral and prokaryotic communities throughout the water column in the (sub)tropical Atlantic Ocean. *The ISME Journal*, *4*(11), 1431–1442. https://doi.org/10.1038/ismej.2010.65

De Corte, D., Sintes, E., Yokokawa, T., Lekunberri, I., & Herndl, G. J. (2016). Large-scale distribution of microbial and viral populations in the South Atlantic Ocean. *Environmental Microbiology Reports*, *8*(2), 305–315. https://doi.org/10.1111/1758-2229.12381

De Corte, D., Sintes, E., Yokokawa, T., Reinthaler, T., & Herndl, G. J. (2012). Links between viruses and prokaryotes throughout the water column along a North Atlantic latitudinal transect. *The ISME Journal*, *6*(8), 1566–1577. https://doi.org/10.1038/ismej.2011.214

Dower, J., Freeland, H., & Juniper, K. (1992). A strong biological response to oceanic flow past Cobb Seamount. *Deep Sea Research Part A. Oceanographic Research Papers*, *39*(7–8), 1139–1145. https://doi.org/10.1016/0198-0149(92)90061-W

Dower, J. F., & Mackas, D. L. (1996). "Seamount effects" in the zooplankton community near Cobb Seamount. *Deep Sea Research Part I: Oceanographic Research Papers*, *43*(6), 837–858. https://doi.org/10.1016/0967-0637(96)00040-4

Dupuy, C., Mallet, C., Guizien, K., Montanié, H., Bréret, M., Mornet, F., … Orvain, F. (2014). Sequential resuspension of biofilm components (viruses, prokaryotes and protists) as measured by erodimetry experiments in the Brouage mudflat (French Atlantic coast). *Journal of Sea Research*, *92*, 56–65. https://doi.org/10.1016/j.seares.2013.12.002

Evans, C., Pearce, I., & Brussaard, C. P. D. (2009). Viral-mediated lysis of microbes and carbon release in the sub-Antarctic and Polar Frontal zones of the Australian Southern Ocean. *Environmental Microbiology*, *11*(11), 2924–2934. https://doi.org/10.1111/j.1462-2920.2009.02050.x

Genin, A. (2004). Bio-physical coupling in the formation of zooplankton and fish aggregations over abrupt topographies. *Journal of Marine Systems*, *50*(1–2), 3–20. https://doi.org/10.1016/j.jmarsys.2003.10.008

Genin, A., & Boehlert, G. W. (1985). Dynamics of temperature and chlorophyll structures above a seamount: An oceanic experiment. *Journal of Marine Research*, *43*(4), 907–924. https://doi.org/10.1357/002224085788453868

Genin, A., & Dower, J. F. (2007). Seamount plankton dynamics. In T. J. Pitcher, T. Morato, P. J. Hart, M. R. Clark, N. Haggan, & R. S. Santos (Eds.), *Seamounts: Ecology, fisheries & conservation* (pp. 85–100). Oxford, UK: Blackwell Publishing. https://doi.org/10.1002/9780470691953

Hassard, F., Gwyther, C. L., Farkas, K., Andrews, A., Jones, V., Cox, B., … Malham, S. (2016). Abundance and distribution of enteric bacteria and viruses in coastal and estuarine sediments—A review. *Frontiers in Microbiology*, https://doi.org/10.3389/fmicb.2016.01692

Hewson, I., O'Neil, J. M., Fuhrman, J. A., & Dennison, W. C. (2001). Virus-like particle distribution and abundance in sediments and overlying waters along eutrophication gradients in two subtropical estuaries. *Limnology and Oceanography*, *46*(7), 1734–1746. https://doi.org/10.4319/lo.2001.46.7.1734

Hu, D., Wu, L., Cai, W., Gupta, A. S., Ganachaud, A., Qiu, B., … Kessler, W. S. (2015). Pacific western boundary currents and their roles in climate. *Nature*, *522*(7556), 299. https://doi.org/10.1038/nature14504

Hwang, C. Y., & Cho, B. C. (2010). Distribution of virus-infected bacteria in the western equatorial Pacific. *Pacific Science*, *64*(2), 177–186. https://doi.org/10.2984/64.2.177

Jiao, N., Herndl, G. J., Hansell, D. A., Benner, R., Kattner, G., Wilhelm, S. W., … Azam, F. (2010). Microbial production of recalcitrant dissolved organic matter: Long-term carbon storage in the global ocean. *Nature Reviews Microbiology*, *8*(8), 593–599. https://doi.org/10.1038/nrmicro2386

Jover, L. F., Effler, T. C., Buchan, A., Wilhelm, S. W., & Weitz, J. S. (2014). The elemental composition of virus particles: Implications for marine biogeochemical cycles. *Nature Reviews Microbiology*, *12*(7), 519–528. https://doi.org/10.1038/nrmicro3289

Lara, E., Vaqué, D., Sà, E. L., Boras, J. A., Gomes, A., Borrull, E., … Duarte, C. M. (2017). Unveiling the role and life strategies of viruses from the surface to the dark ocean. *Science Advances*, *3*(9), e1602565. https://doi.org/10.1126/sciadv.1602565

Larsen, A., Castberg, T., Sandaa, R. A., Brussaard, C. P. D., Egge, J., Heldal, M., … Bratbak, G. (2001). Population dynamics and diversity of phytoplankton, bacteria and viruses in a seawater enclosure. *Marine Ecology Progress Series*, *221*, 47–57. https://doi.org/10.3354/meps221047

Larsen, A., Flaten, G. A. F., Sandaa, R.-A., Castberg, T., Thyrhaug, R., Erga, S. R., … Bratbak, G. (2004). Spring phytoplankton bloom dynamics in Norwegian coastal waters: Microbial community succession and diversity. *Limnology and Oceanography*, *49*(1), 180–190. https://doi.org/10.4319/lo.2004.49.1.0180

Larsen, J. B., Larsen, A., Thyrhaug, R., Bratbak, G., & Sandaa, R.-A. (2008). Response of marine viral populations to a nutrient induced phytoplankton bloom at different $pCO_2$ levels. *Biogeosciences*, *5*(2), 523–533. https://doi.org/10.5194/bg-5-523-2008

Li, Y., Luo, T., Sun, J., Cai, L., Liang, Y., Jiao, N., & Zhang, R. (2014). Lytic viral infection of bacterioplankton in deep waters of the western Pacific Ocean. *Biogeosciences*, *11*(9), 2531–2542. https://doi.org/10.5194/bg-11-2531-2014

Liang, Y., Li, L., Luo, T., Zhang, Y., Zhang, R., & Jiao, N. (2014). Horizontal and vertical distribution of marine virioplankton: A basin scale investigation based on a global cruise. *PLoS ONE*, *9*(11), e111634. https://doi.org/10.1371/journal.pone.0111634

Liang, Y., Zhang, Y., Zhang, Y., Luo, T., Rivkin, R. B., & Jiao, N. (2017). Distributions and relationships of virio-and picoplankton in the epi-, meso-and bathypelagic zones of the Western Pacific Ocean. *FEMS Microbiology Ecology*, *93*(2), fiw238. https://doi.org/10.1093/femsec/fiw238

Longhurst, A. R. (2007). *Ecological geography of the sea* (2nd ed.). San Diego, CA: Academic Press. https://doi.org/10.1016/B978-0-12-455521-1.X5000-1

Lymer, D., & Vrede, K. (2006). Nutrient additions resulting in phage release and formation of non-nucleoid-containing bacteria. *Aquatic Microbial Ecology*, *43*(2), 107–112. https://doi.org/10.3354/ame043107

Magiopoulos, I., & Pitta, P. (2012). Viruses in a deep oligotrophic sea: Seasonal distribution of marine viruses in the epi-, meso- and bathypelagic waters of the Eastern Mediterranean Sea. *Deep Sea Research Part I: Oceanographic Research Papers*, *66*, 1–10. https://doi.org/10.1016/j.dsr.2012.03.009

Marie, D., Brussaard, C. P., Thyrhaug, R., Bratbak, G., & Vaulot, D. (1999). Enumeration of marine viruses in culture and natural samples by flow cytometry. *Applied and Environmental Microbiology*, *65*(1), 45–52.

Marie, D., Partensky, F., Vaulot, D., & Brussaard, C. (1999). Enumeration of phytoplankton, bacteria, and viruses in marine samples. *Current Protocols in Cytometry*, *10*(1), 1–11. https://doi.org/10.1002/047142956.cy1111s10

Marie, D., Simon, N., Guillou, L., Partensky, F., & Vaulot, D. (2000). Flow cytometry analysis of marine picoplankton. In R. A. Diamond, & S. DeMaggio (Eds.), *In living color: Protocols in flow cytometry and cell sorting* (pp. 421–454). New York, NY: Springer-Verlag, Berlin Heidelberg. https://doi.org/10.1007/978-3-642-57049-0_34

Martínez, J. M., Swan, B. K., & Wilson, W. H. (2014). Marine viruses, a genetic reservoir revealed by targeted viromics. *The ISME Journal*, *8*(5), 1079–1088. https://doi.org/10.1038/ismej.2013.214

Maurice, C. F., Bouvier, C., de Wit, R., & Bouvier, T. (2013). Linking the lytic and lysogenic bacteriophage cycles to environmental conditions, host physiology and their variability in coastal lagoons. *Environmental Microbiology*, *15*(9), 2463–2475. https://doi.org/10.1111/1462-2920.12120

Mendonça, A., Arístegui, J., Vilas, J. C., Montero, M. F., Ojeda, A., Espino, M., & Martins, A. (2012). Is there a seamount effect on microbial community structure and biomass? The case study of Seine and Sedlo Seamounts (Northeast Atlantic). *PLoS ONE*, *7*(1), e29526. https://doi.org/10.1371/journal.pone.0029526

Mojica, K. D. A., & Brussaard, C. P. D. (2014). Factors affecting virus dynamics and microbial host-virus interactions in marine environments. *FEMS Microbiology Ecology*, *89*(3), 495–515. https://doi.org/10.1111/1574-6941.12343

Mojica, K. D. A., Huisman, J., Wilhelm, S. W., & Brussaard, C. P. D. (2016). Latitudinal variation in virus-induced mortality of phytoplankton across the North Atlantic Ocean. *The ISME Journal*, *10*(2), 500–513. https://doi.org/10.1038/ismej.2015.130

Montserrat, F., Guilhon, M., Corrêa, P. V. F., Bergo, N. M., Signori, C. N., Tura, P. M., … Turra, A. (2019). Deep-sea mining on the Rio Grande Rise (Southwestern Atlantic): A review on environmental baseline, ecosystem services and potential impacts. *Deep Sea Research Part I: Oceanographic Research Papers*, *145*, 31–58. https://doi.org/10.1016/j.dsr.2018.12.007

Mouriño, B., Fernández, E., Pingree, R., Sinha, B., Escánez, J., & de Armas, D. (2005). Constraining effect of mesoscale features on carbon budget of photic layer in the NE subtropical Atlantic. *Marine Ecology Progress Series*, *287*, 45–52. https://doi.org/10.3354/meps287045

Muck, S., Griessler, T., Köstner, N., Klimiuk, A., Winter, C., & Herndl, G. J. (2014). Fracture zones in the Mid Atlantic Ridge lead to alterations in prokaryotic and viral parameters in deep-water masses. *Frontiers in Microbiology*, *5*, 264. https://doi.org/10.3389/fmicb.2014.00264

Partensky, F., Blanchot, J., & Vaulot, D. (1999). Differential distribution and ecology of *Prochlorococcus* and *Synechococcus* in oceanic waters: A review. *Bulletin-Institut Oceanographique Monaco-Numero Special*, *19*, 457–475.

Paterson, J. S., Nayar, S., Mitchell, J. G., & Seuront, L. (2012). A local upwelling controls viral and microbial community structure in South Australian continental shelf waters. *Estuarine, Coastal and Shelf Science*, *96*, 197–208. https://doi.org/10.1016/j.ecss.2011.11.009

Payet, J. P., McMinds, R., Burkepile, D. E., & Vega Thurber, R. L. (2014). Unprecedented evidence for high viral abundance and lytic activity in coral reef waters of the South Pacific Ocean. *Frontiers in Microbiology*, *5*, 493. https://doi.org/10.3389/fmicb.2014.00493

Read, J., & Pollard, R. (2017). An introduction to the physical oceanography of six seamounts in the southwest Indian Ocean. *Deep Sea Research Part II: Topical Studies in Oceanography*, *136*, 44–58. https://doi.org/10.1016/j.dsr2.2015.06.022

Roden, G. I. (1987). Effect of seamounts and seamount chains on ocean circulation and thermohaline structure. In B. H. Keating, P. Fryer, R. Batiza, G. W. Boehlert (Eds.), *Effect of seamounts and seamount chains on ocean circulation and thermohaline structure* (Vol. *43*, pp. 335–354). Washington, DC: American Geophysical Union. https://doi.org/10.1029/GM043p0335

Rogers, A. D. (2018). The biology of seamounts: 25 Years on. In C. Sheppard (Ed.), *Advances in marine biology* (Vol. *79*, pp. 137–224). London, UK: Academic Press. https://doi.org/10.1016/bs.amb.2018.06.001

Rogers, A. D., Brierley, A., Croot, P., Cunha, M. R., Danovaro, R., Devey, C., … Trevisanut, S. (2015). Delving deeper: Critical challenges for 21st century deep-sea research. In K. E. Larkin, K. Donaldson, & N. McDonough (Eds.), *Position paper 22 of the European Marine Board* (Vol. *22*, pp. 224). Ostend, Belgium: European Marine Board.

Rowden, A. A., Dower, J. F., Schlacher, T. A., Consalvey, M., & Clark, M. R. (2010). Paradigms in seamount ecology: Fact, fiction and future. *Marine Ecology*, *31*, 226–241. https://doi.org/10.1111/j.1439-0485.2010.00400.x

Rowe, J. M., DeBruyn, J. M., Poorvin, L., LeCleir, G. R., Johnson, Z. I., Zinser, E. R., & Wilhelm, S. W. (2012). Viral and bacterial abundance

and production in the Western Pacific Ocean and the relation to other oceanic realms. *FEMS Microbiology Ecology*, *79*(2), 359–370. https://doi.org/10.1111/j.1574-6941.2011.01223.x

Sampaio de Souza, C., Guimarães da Luz, J. A., Macedo, S., Montes, M. D. J. F., & Mafalda, P. (2013). Chlorophyll *a* and nutrient distribution around seamounts and islands of the tropical south-western Atlantic. *Marine and Freshwater Research*, *64*(2), 168–184. https://doi.org/10.1071/mf12075

Sime-Ngando, T., Juniper, K., & Vézina, A. (1992). Ciliated protozoan communities over Cobb Seamount: Increase in biomass and spatial patchiness. *Marine Ecology Progress Series*, *89*(1), 37–51. https://doi.org/10.3354/meps089037

Sonnekus, M. J., Bornman, T. G., & Campbell, E. E. (2017). Phytoplankton and nutrient dynamics of six South West Indian Ocean seamounts. *Deep Sea Research Part II: Topical Studies in Oceanography*, *136*, 59–72. https://doi.org/10.1016/j.dsr2.2016.12.008

Suttle, C. A. (1994). The significance of viruses to mortality in aquatic microbial communities. *Microbial Ecology*, *28*(2), 237–243. https://doi.org/10.1007/BF00166813

Suttle, C. A. (2007). Marine viruses—Major players in the global ecosystem. *Nature Reviews Microbiology*, *5*(10), 801–812. https://doi.org/10.1038/nrmicro1750

Suttle, C. A. (2016). Environmental microbiology: Viral diversity on the global stage. *Nature Microbiology*, *1*, 16205. https://doi.org/10.1038/nmicrobiol.2016.205

Toole, J. M., Zou, E., & Millard, R. C. (1988). On the circulation of the upper waters in the western equatorial Pacific Ocean. *Deep Sea Research Part A. Oceanographic Research Papers*, *35*(9), 1451–1482. https://doi.org/10.1016/0198-0149(88)90097-0

Wei, W., Zhang, R., Peng, L., Liang, Y., & Jiao, N. (2018). Effects of temperature and photosynthetically active radiation on virioplankton decay in the western Pacific Ocean. *Scientific Reports*, *8*(1), 1525. https://doi.org/10.1038/s41598-018-19678-3

Weitz, J. S., & Wilhelm, S. W. (2012). Ocean viruses and their effects on microbial communities and biogeochemical cycles. *F1000 Biology Reports*, *4*, 17. https://doi.org/10.3410/B4-17

White, M., Bashmachnikov, I., Arístegui, J., & Martins, A. (2007). Physical processes and seamount productivity. In T. J. Pitcher, T. Morato, P. J. B. Hart, M. R. Clark, N. Haggan, R. S. Santos (Eds.), *Seamounts: Ecology, fisheries & conservation* (pp. 65–84). Oxford, UK: Wiley Online Library. https://doi.org/10.1002/9780470691953

Wigington, C. H., Sonderegger, D., Brussaard, C. P. D., Buchan, A., Finke, J. F., Fuhrman, J. A., … Weitz, J. S. (2016). Re-examination of the relationship between marine virus and microbial cell abundances. *Nature Microbiology*, *1*(3), nmicrobiol201524. https://doi.org/10.1038/nmicrobiol.2015.24

Wilhelm, S. W., Brigden, S. M., & Suttle, C. A. (2002). A dilution technique for the direct measurement of viral production: A comparison in stratified and tidally mixed coastal waters. *Microbial Ecology*, *43*(1), 168–173. https://doi.org/10.1007/s00248-001-1021-9

Williamson, S. J., Houchin, L. A., McDaniel, L., & Paul, J. H. (2002). Seasonal variation in lysogeny as depicted by prophage induction in Tampa Bay, Florida. *Applied and Environmental Microbiology*, *68*(9), 4307–4314. https://doi.org/10.1128/AEM.68.9.4307-4314.2002

Williamson, S. J., & Paul, J. H. (2004). Nutrient stimulation of lytic phage production in bacterial populations of the Gulf of Mexico. *Aquatic Microbial Ecology*, *36*(1), 9–17. https://doi.org/10.3354/ame036009

Winter, C., Kerros, M.-E., & Weinbauer, M. G. (2009). Seasonal and depth-related dynamics of prokaryotes and viruses in surface and deep waters of the northwestern Mediterranean Sea. *Deep Sea Research Part I: Oceanographic Research Papers*, *56*(11), 1972–1982. https://doi.org/10.1016/j.dsr.2009.07.003

Winter, C., Köstner, N., Kruspe, C. P., Urban, D., Muck, S., Reinthaler, T., & Herndl, G. J. (2018). Mixing alters the lytic activity of viruses in the dark ocean. *Ecology*, *99*(3), 700–713. https://doi.org/10.1002/ecy.2135

Wommack, K. E., & Colwell, R. R. (2000). Virioplankton: Viruses in aquatic ecosystems. *Microbiology and Molecular Biology Reviews*, *64*(1), 69–114. https://doi.org/10.1128/mmbr.64.1.69-114.2000

Yang, Y., & Jiao, N. (2002). Distribution of virioplankton in the Kuroshio Current and the adjacent area in the East China Sea as determined by flow cytometry. *Chinese Journal of Oceanology and Limnology*, *20*(Special Issue), 1–7.

Yang, Y., Motegi, C., Yokokawa, T., & Nagata, T. (2010). Large-scale distribution patterns of virioplankton in the upper ocean. *Aquatic Microbial Ecology*, *60*(3), 233–246. https://doi.org/10.3354/ame01428

Yang, Y., Yokokawa, T., Motegi, C., & Nagata, T. (2014). Large-scale distribution of viruses in deep waters of the Pacific and Southern Oceans. *Aquatic Microbial Ecology*, *71*(3), 193–202. https://doi.org/10.3354/ame01677

Yesson, C., Clark, M. R., Taylor, M. L., & Rogers, A. D. (2011). The global distribution of seamounts based on 30 arc seconds bathymetry data. *Deep Sea Research Part I: Oceanographic Research Papers*, *58*(4), 442–453. https://doi.org/10.1016/j.dsr.2011.02.004

Zhang, R., Wei, W., & Cai, L. (2014). The fate and biogeochemical cycling of viral elements. *Nature Reviews Microbiology*, *12*(12), 850–851. https://doi.org/10.1038/nrmicro3384

Zhang, W.-J., Sun, X.-X., Chen, Y.-Y., Li, J.-L., & Du, J. (2016). Chlorophyll a concentration and size structure of phytoplankton at Yarp Y3 seamount in tropical West Pacific in winter 2014. *Oceanologia Et Limnologia Sinica*, *47*(4), 739–747 (In Chinese with English abstract). https://doi.org/10.11693/hyhz20160100020

Zhao, L., Zhao, Y.-C., Wang, C.-F., Zhang, W.-C., Sun, X.-X., Li, X.-G., … Xiao, T. (2017). Comparison in the distribution of microbial food web components in the Y3 and M2 seamounts in the tropical western Pacific. *Oceanologia Et Limnologia Sinica*, *48*(6), 1446–21455 (In Chinese with English abstract). https://doi.org/10.11693/hyhz20170600160

**How to cite this article:** Zhao Y, Zhao Y, Zheng S, et al. Virioplankton distribution in the tropical western Pacific Ocean in the vicinity of a seamount. *MicrobiologyOpen*. 2020;9:e1031. https://doi.org/10.1002/mbo3.1031

## APPENDIX

**TABLE A1** Sampling stations and sample depths

| | Station | Latitude (°N) | Longitude (°E) | Depth (m) | Sampled depths (m) |
|---|---|---|---|---|---|
| Seamount stations | 0 | 10.4769 | 140.1347 | 110 | 3, 15, 30, 50, 75, 101 |
| | 1 | 10.4335 | 140.1483 | 57 | 3, 15, 30, 50 |
| | 2 | 10.4081 | 140.1569 | 1,140 | 3, 30, 50, 75, 118, 150, 200, 300, 500, 1,130 |
| | 3 | 10.3706 | 140.1684 | 1,465 | 3, 30, 50, 75, 128, 150, 200, 300, 500, 1,000, 1,450 |
| | 5 | 10.5233 | 140.1194 | 92 | 3, 15, 30, 50, 87 |
| | 6 | 10.5601 | 140.1179 | 932 | 3, 30, 50, 75, 115, 150, 200, 300, 500, 920 |
| | 11 | 10.4762 | 140.1118 | 615 | 3, 30, 50, 75, 100, 133, 200, 300, 610 |
| | 12 | 10.4754 | 140.0921 | 1,555 | 3, 30, 50, 75, 119, 150, 200, 300, 500, 1,000, 1,540 |
| | 17 | 10.4807 | 140.1575 | 506 | 3, 30, 50, 75, 100, 126, 200, 300, 500 |
| | 18 | 10.4886 | 140.1898 | 1,716 | 3, 30, 50, 75, 120, 150, 200, 300, 500, 1,000, 1,700 |
| Far-field stations | 4 | 10.3040 | 140.1898 | 1,521 | 3, 30, 50, 75, 120, 150, 200, 300, 500, 1,000, 1,506 |
| | 7 | 10.6199 | 140.1192 | 2,368 | 3, 30, 50, 75, 100, 136, 200, 300, 500, 1,000, 2,340 |
| | 8 | 10.6628 | 140.1218 | 3,508 | 3, 30, 50, 75, 100, 128, 200, 300, 500, 1,000, 2,000, 3,490 |
| | 9 | 10.7213 | 140.1205 | 4,512 | 3, 30, 50, 75, 100, 138, 200, 300, 500, 1,000, 2,000, 4,501 |
| | 10 | 10.9138 | 140.0889 | 5,999 | 3, 30, 50, 75, 100, 138, 200, 300, 500, 1,000, 2,000, 4,000, 5,950 |
| | 13 | 10.4738 | 140.0629 | 2,211 | 3, 30, 50, 75, 112, 150, 200, 300, 500, 1,000, 2,190 |
| | 14 | 10.4717 | 140.0029 | 2,297 | 3, 30, 50, 75, 119, 150, 200, 300, 500, 1,000, 2,271, |
| | 15 | 10.4696 | 139.9285 | 2,778 | 3, 30, 50, 75, 100, 150, 200, 300, 500, 1,000, 2,763 |
| | 16 | 10.4688 | 139.8599 | 2,760 | 3, 30, 50, 75, 100, 136, 200, 300, 500, 1,000, 2,000, 2,730 |
| | 19 | 10.4973 | 140.2264 | 2,500 | 3, 30, 50, 75, 100, 132, 200, 300, 500, 1,000, 2,000, 2,470 |
| | 20 | 10.5117 | 140.2862 | 2,731 | 3, 30, 50, 75, 100, 131, 200, 300, 500, 1,000, 2,000, 2,700 |
| | 21 | 10.5329 | 140.3765 | 2,477 | 3, 30, 50, 75, 100, 131, 200, 300, 500, 1,000, 2,000, 2,448 |

**TABLE A2** Sampling stations and sample depths for seamount and far-field stations in upper 75 m water column

| | Station | Latitude (°N) | Longitude (°E) | Sampled depths (m) |
|---|---|---|---|---|
| Seamount stations | 0 | 10.4769 | 140.1347 | 3, 15, 30, 50, 75 |
| | 1 | 10.4335 | 140.1483 | 3, 15, 30, 50 |
| | 2 | 10.4081 | 140.1569 | 3, 30, 50, 75 |
| | 3 | 10.3706 | 140.1684 | 3, 30, 50, 75 |
| | 5 | 10.5233 | 140.1194 | 3, 15, 30, 50 |
| | 6 | 10.5601 | 140.1179 | 3, 30, 50, 75 |
| | 11 | 10.4762 | 140.1118 | 3, 30, 50, 75 |
| | 12 | 10.4754 | 140.0921 | 3, 30, 50, 75 |
| | 17 | 10.4807 | 140.1575 | 3, 30, 50, 75 |
| | 18 | 10.4886 | 140.1898 | 3, 30, 50, 75 |
| Far-field stations | 4 | 10.3040 | 140.1898 | 3, 30, 50, 75 |
| | 7 | 10.6199 | 140.1192 | 3, 30, 50, 75 |
| | 8 | 10.6628 | 140.1218 | 3, 30, 50, 75 |
| | 9 | 10.7213 | 140.1205 | 3, 30, 50, 75 |
| | 10 | 10.9138 | 140.0889 | 3, 30, 50, 75 |
| | 13 | 10.4738 | 140.0629 | 3, 30, 50, 75 |
| | 14 | 10.4717 | 140.0029 | 3, 30, 50, 75 |
| | 15 | 10.4696 | 139.9285 | 3, 30, 50, 75 |
| | 16 | 10.4688 | 139.8599 | 3, 30, 50, 75 |
| | 19 | 10.4973 | 140.2264 | 3, 30, 50, 75 |
| | 20 | 10.5117 | 140.2862 | 3, 30, 50, 75 |
| | 21 | 10.5329 | 140.3765 | 3, 30, 50, 75 |

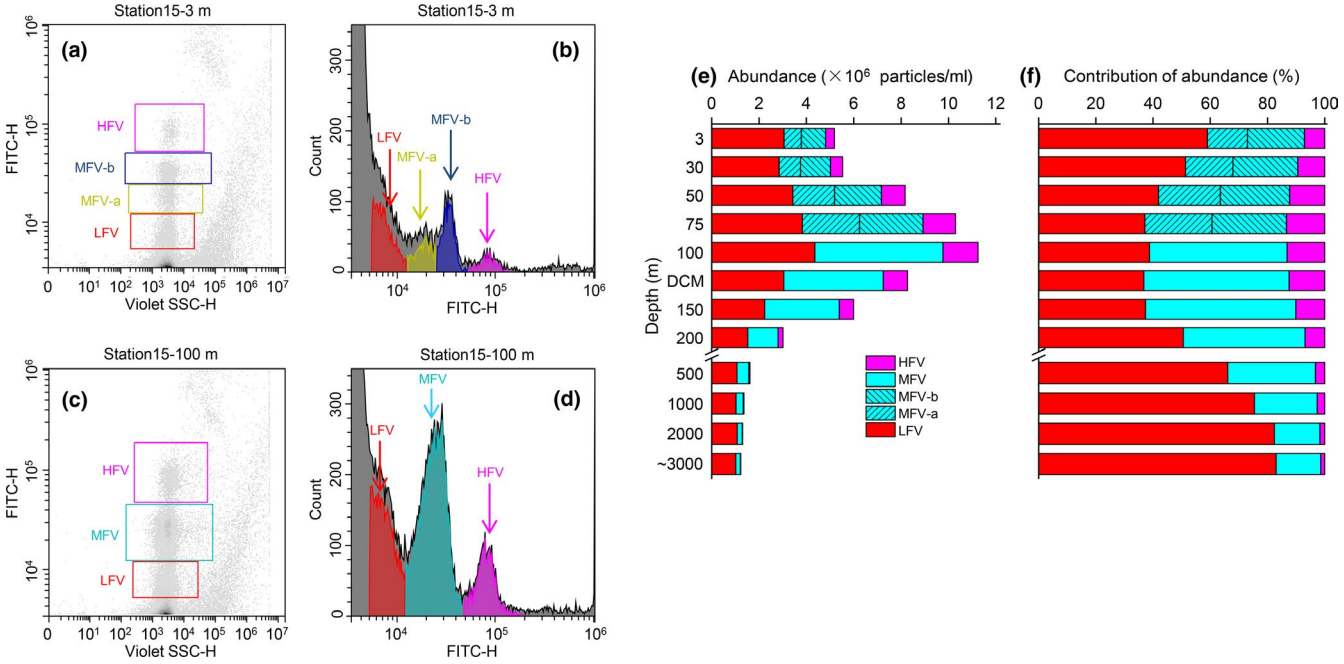



**FIGURE A1** Viral subcluster cytograms (a–d), vertical abundance profile for various subclusters (e), and their contributions to total viral abundance (f). (a, b) Sample cytograms of four viral subclusters in upper 75 m layers; (c, d) sample cytograms of three viral subclusters in 100 m and deeper layers. HFV, high fluorescence viruses; LFV, low fluorescence viruses; MFV, medium fluorescence viruses, MFV classified as subclusters MFV-a and MFV-b in upper 75 m layers. Indicated abundances are averages for all stations. Figures a-d created in Beckman Coulter CytExpert, v. 2.3.0.84 https://www.beckman.com/flow-cytometry/instruments/cytoflex/software. Figures e and f created in OriginLab Origin v. 8.5 https://www.originlab.com/

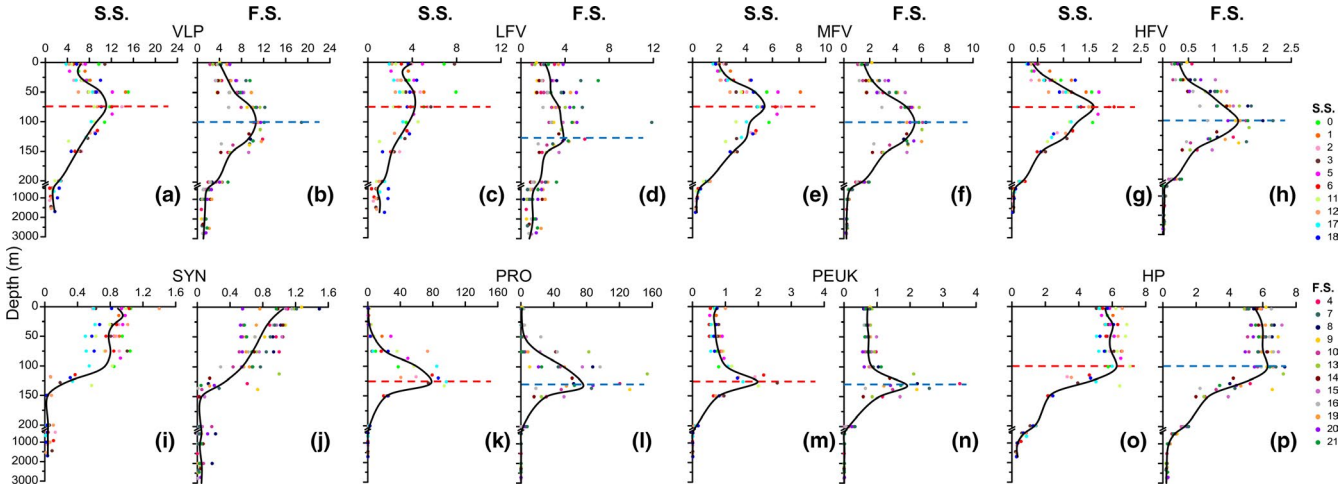



**FIGURE A2** Vertical virioplankton and picoplankton distributions in seamount and far-field stations. F.S., far-field stations; S.S., seamount stations. Colored dots show virioplankton and picoplankton abundances. Black lines show average virioplankton and picoplankton abundances in seamount and far-field stations. Red and blue dotted lines show maximum abundance depths in seamount and far-field stations, respectively. HFV, high fluorescence viruses, $\times 10^6$ particles/ml; HP, heterotrophic prokaryotes, $\times 10^5$ cells/ml; LFV, low fluorescence viruses, $\times 10^6$ particles/ml; MFV, medium fluorescence viruses, $\times 10^6$ particles/ml; PEUK, picoeukaryotes, $\times 10^3$ cells/ml; PRO, *Prochlorococcus*, $\times 10^3$ cells/ml; SYN, *Synechococcus*, $\times 10^3$ cells/ml; VLP, virus-like particles, $\times 10^6$ particles/ml. Figures created in Golden Software Grapher v. 8.5 https://www.goldensoftware.com/products/grapher

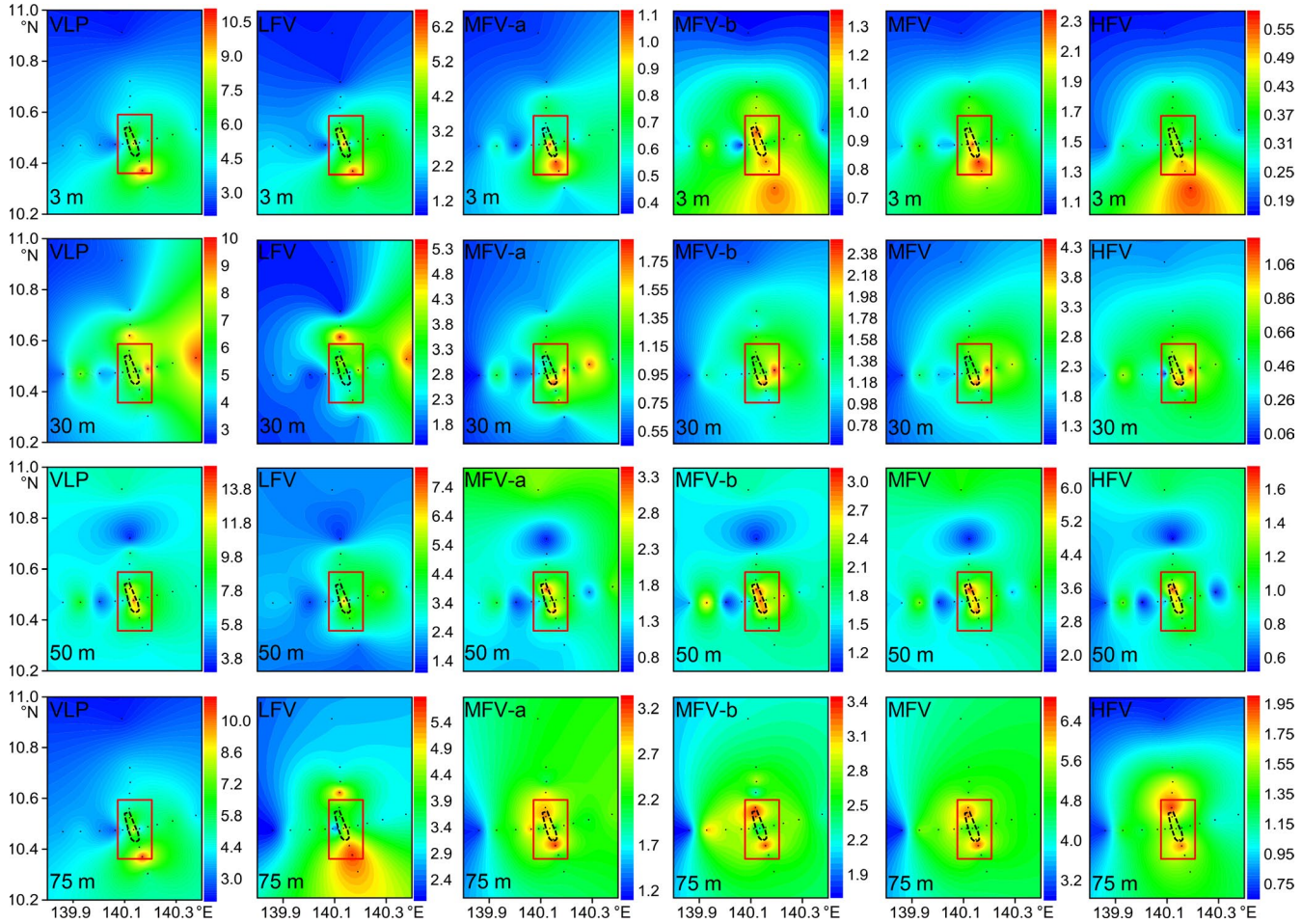



**FIGURE A3** Horizontal virioplankton abundance distributions in the upper 75 m water column. Dotted black lines indicate the location of Caroline Seamount summit. Seamount stations are inside the red rectangle. Others are far-field stations. HFV, high fluorescence viruses, $\times 10^6$ particles/ml; LFV, low fluorescence viruses, $\times 10^6$ particles/ml; MFV, medium fluorescence viruses, $\times 10^6$ particles/ml, MFV classified as subclusters MFV-a and MFV-b in upper 75 m layers; VLP, virus-like particles, $\times 10^6$ particles/ml. Figures created in Golden Software Surfer v. 13 https://www.goldensoftware.com/products/surfer